First next-to-next-to-leading-order extraction of fragmentation functions for Λ hyperons

Valerio Bertone, **Alessia Bongallino**, Amedeo Chiefa,
Miguel G. Echevarría, Gunar Schnell

Based on arXiv:2605.05314

QCD Evolution 2026

May 11th, 2026

EHU | Qc EHU Quantum Center

Universality of FFs

Collinear unpolarised FFs are the most extensively studied FFs

Their determination has improved significantly in recent years, driven by the availability of new experimental measurements and by increasingly accurate calculation of partonic cross sections

Universality of FFs

Collinear unpolarised FFs are the most extensively studied FFs

Their determination has improved significantly in recent years, driven by the availability of new experimental measurements and by increasingly accurate calculation of partonic cross sections

Single-inclusive annihilation

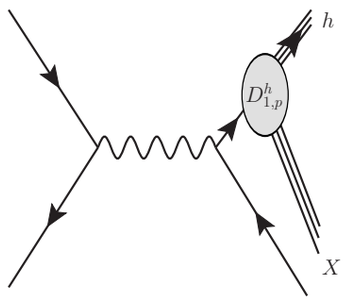

Semi-inclusive deep-inelastic scattering

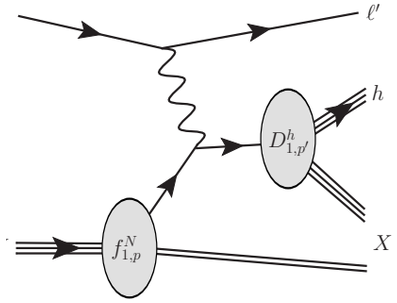

Inclusive hadron production in pp collisions

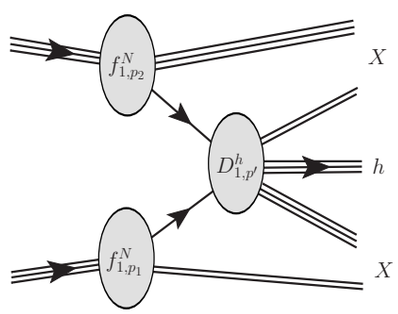

Universality of FFs

Collinear unpolarised FFs are the most extensively studied FFs

Their determination has improved significantly in recent years, driven by the availability of new experimental measurements and by increasingly accurate calculation of partonic cross sections

Single-inclusive annihilation

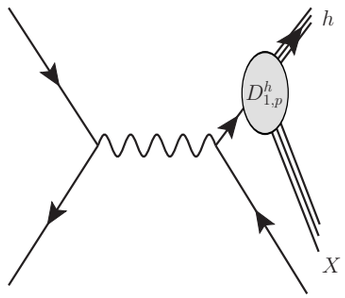

Semi-inclusive deep-inelastic scattering

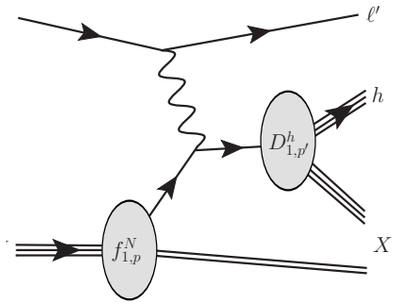

Inclusive hadron production in pp collisions

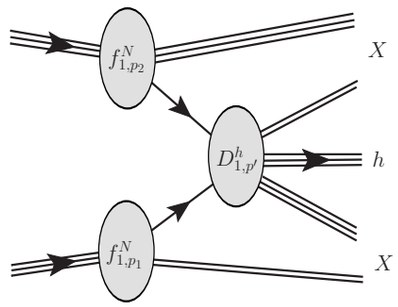

Factorisation of the cross section

$$d\sigma^{e^+e^-\to hX} \propto d\hat{\sigma} \otimes D^h_{1,p}$$

$$d\sigma^{\ell N\to \ell' hX} \propto d\hat{\sigma} \otimes f^N_{1,p} \otimes D^h_{1,p'}$$

$$d\sigma^{pp\to hX} \propto d\hat{\sigma} \otimes f^N_{1,p_1} \otimes f^N_{1,p_2} \otimes D^h_{1,p'}$$

Universality of FFs

Collinear unpolarised FFs are the most extensively studied FFs

Their determination has improved significantly in recent years, driven by the availability of new experimental measurements and by increasingly accurate calculation of partonic cross sections

Single-inclusive annihilation

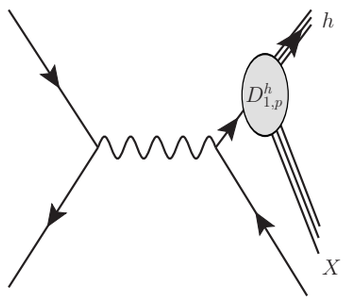

Semi-inclusive deep-inelastic scattering

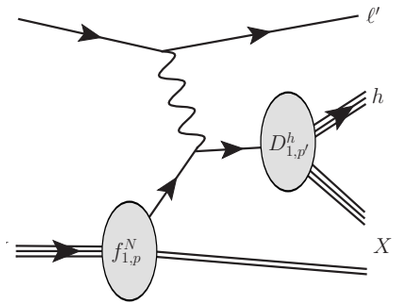

Inclusive hadron production in pp collisions

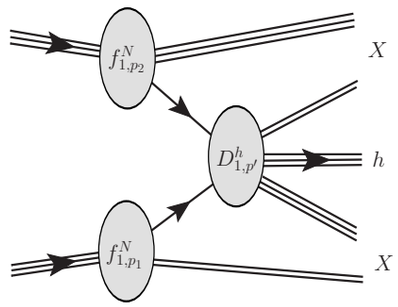

Factorisation of the cross section

$d\sigma^{e^+e^-\to hX} \propto d\hat{\sigma} \otimes D^h_{1,p}$

$d\sigma^{\ell N\to \ell' hX} \propto d\hat{\sigma} \otimes f^N_{1,p} \otimes D^h_{1,p'}$

$d\sigma^{pp\to hX} \propto d\hat{\sigma} \otimes f^N_{1,p_1} \otimes f^N_{1,p_2} \otimes D^h_{1,p'}$

Flavour sensitivity

$D^h_{1,q} + D^h_{1,\bar{q}}$

$D^h_{1,q}$

$D^h_{1,q}$

Universality of FFs

Collinear unpolarised FFs are the most extensively studied FFs

Their determination has improved significantly in recent years, driven by the availability of new experimental measurements and by increasingly accurate calculation of partonic cross sections

Single-inclusive annihilation

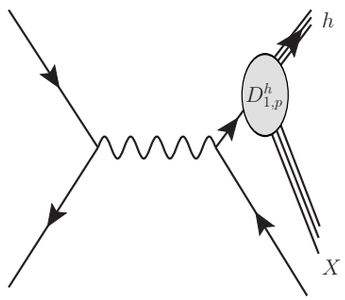

Semi-inclusive deep-inelastic scattering

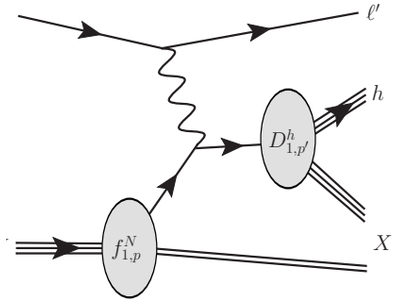

Inclusive hadron production in pp collisions

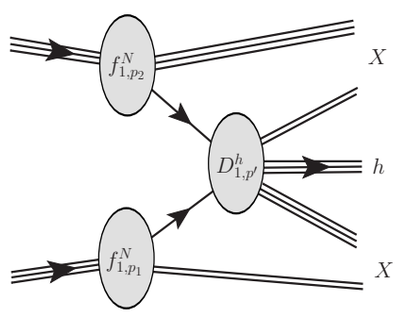

Factorisation of the cross section

$d\sigma^{e^+e^-\to hX} \propto d\hat{\sigma} \otimes D^h_{1,p}$

$d\sigma^{\ell N\to \ell' hX} \propto d\hat{\sigma} \otimes f^N_{1,p} \otimes D^h_{1,p'}$

$d\sigma^{pp\to hX} \propto d\hat{\sigma} \otimes f^N_{1,p_1} \otimes f^N_{1,p_2} \otimes D^h_{1,p'}$

Flavour sensitivity

$D^h_{1,q} + D^h_{1,\bar{q}}$

$D^h_{1,q}$

$D^h_{1,q}$

NNLO perturbative corrections

P. J. Rijken and W. L. van Neerven, Phys. Lett. B 386 (1996) 422–428
P. J. Rijken and W. L. van Neerven, Nucl. Phys. B 487 (1997) 233–282
P. J. Rijken and W. L. van Neerven, Phys. Lett. B 392 (1997) 207–215
J. Blümlein and V. Ravindran, Nucl. Phys. B 749 (2006) 1–24
A. Mitov and S.-O. Moch, Nucl. Phys. B 751 (2006) 18–52

L. Bonino, et al., Phys. Rev. Lett. 132 (2024) 251901
S. Goyal et al., Phys. Rev. Lett. 132 (2024) 251902
L. Bonino, et al., JHEP 10 (2025) 016
S. Goyal et al., Phys. Rev. D 111 (2025) 094007
S. Goyal et al., arXiv: 2603.30012

M. Czakon T. Generet, A. Mitov, and R. Poncelet, Phys. Rev. Lett. 135 (2025) 17

Motivation

Improving the determination of FFs by focusing on a less extensively explored hadron:
the Λ hyperon, the lightest among the strange baryons

Motivation

Improving the determination of FFs by focusing on a less extensively explored hadron: the Λ hyperon, the lightest among the strange baryons

State of the art of Λ collinear unpolarised fits

Collaboration	Data	Flavour separation	Accuracy	Extracted particle
DSV (1998) Phys. Rev. D 57, 5811	SIA	$u = d = s$	NLO	$\Lambda + \bar{\Lambda}$
AKK (2006) Nucl. Phys. B, 734	SIA	✓		
(2008) Nucl. Phys. B 803	SIA, pp collisions	✓		
NPC23 (2025) Phys. Rev. D 112, 054045	SIA, SIDIS, pp collisions	$u = d$		

Motivation

Improving the determination of FFs by focusing on a less extensively explored hadron: the Λ hyperon, the lightest among the strange baryons

State of the art of Λ collinear unpolarised fits

Collaboration	Data	Flavour separation	Accuracy	Extracted particle
DSV (1998) Phys. Rev. D 57, 5811	SIA	$u = d = s$	NLO	$\Lambda + \bar{\Lambda}$
AKK (2006) Nucl. Phys. B, 734	SIA	✓		
(2008) Nucl. Phys. B 803	SIA, pp collisions	✓		
NPC23 (2025) Phys. Rev. D 112, 054045	SIA, SIDIS, pp collisions	$u = d$		
MAPFF1.0_Λ (2026)	SIA, SIDIS (NC and CC)	✓	NNLO	$\Lambda, \bar{\Lambda}$

Motivation

Improving the determination of FFs by focusing on a less extensively explored hadron: the Λ hyperon, the lightest among the strange baryons

State of the art of Λ collinear unpolarised fits

Collaboration	Data	Flavour separation	Accuracy	Extracted particle
DSV (1998) Phys. Rev. D 57, 5811	SIA	$u = d = s$		
	IA	✓		
	A, llisions	✓	NLO	$\Lambda + \bar{\Lambda}$
NPC23 (2025) Phys. Rev. D 112, 054045	SIA, SIDIS, pp collisions	$u = d$		
MAPFF1.0_Λ (2026)	SIA, SIDIS (NC and CC)	✓	NNLO	$\Lambda, \bar{\Lambda}$

Inclusion of all available SIDIS neutral-and – for the first time – **charged-current** data

Motivation

Improving the determination of FFs by focusing on a less extensively explored hadron: the Λ hyperon, the lightest among the strange baryons

State of the art of Λ collinear unpolarised fits

Collaboration	Data	Flavour separation	Accuracy	Extracted particle
DSV (1998) Phys. Rev. D 57, 5811	SIA	$u = d = s$		
	IA	✓		
	A, llisions	✓		
NPC23 (2025) Phys. Rev. D 112, 054045	SIA, SIDIS, pp collisions	$u = d$		
MAPFF1.0_Λ (2026)	SIA, SIDIS (NC and CC)	✓	NNLO	$\Lambda, \bar{\Lambda}$

Inclusion of all available SIDIS neutral-and – for the first time – **charged-current** data

SIDIS data allow to reliably extract for the first time FFs for Λ and $\bar{\Lambda}$ **separately**

Motivation

Improving the determination of FFs by focusing on a less extensively explored hadron: the Λ hyperon, the lightest among the strange baryons

State of the art of Λ collinear unpolarised fits

Collaboration	Data	Flavour separation	Accuracy	Extracted particle
DSV (1998) Phys. Rev. D 57, 5811	SIA	$u = d = s$		
NPC23 (2025) Phys. Rev. D 112, 054045	SIA, SIDIS, pp collisions	$u = d$		
MAPFF1.0_Λ (2026)	SIA, SIDIS (NC and CC)	✓	NNLO	$\Lambda, \bar{\Lambda}$

Inclusion of all available SIDIS neutral-and – for the first time – **charged-current** data

First independent determination of valence-quark distribution for the Λ, i.e., for u, d, s

SIDIS data allow to reliably extract for the first time FFs for Λ and $\bar{\Lambda}$ **separately**

Theoretical framework

Theoretical framework

Single-inclusive annihilation

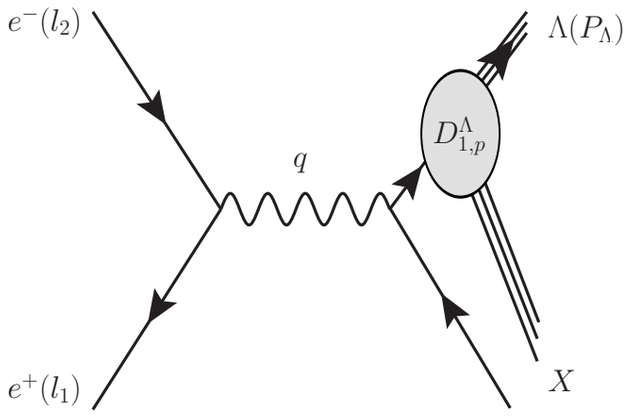

$$\frac{d\sigma^h}{dz} = \frac{4\pi\alpha^2(Q)}{Q^2} F_2^h(z,Q)$$

$$F_2^h(z,Q) = \frac{1}{n_f}\sum_q^{n_f} \hat{e}_q^2(Q)\Big[C_{2,q}^S\left(z,\alpha_s(Q)\right)\otimes D_{1,\Sigma}^h\left(z,Q\right) + C_{2,q}^{NS}\left(z,\alpha_s(Q)\right)\otimes D_{1,NS}^h\left(z,Q\right) + C_{2,g}^S\left(z,\alpha_s(Q)\right)\otimes D_{1,g}^h\left(z,Q\right)\Big]$$

P. J. Rijken and W. L. van Neerven, Phys. Lett. B 386 (1996) 422–428
P. J. Rijken and W. L. van Neerven, Nucl. Phys. B 487 (1997) 233–282
P. J. Rijken and W. L. van Neerven, Phys. Lett. B 392 (1997) 207–215
J. Blümlein and V. Ravindran, Nucl. Phys. B 749 (2006) 1–24
A. Mitov and S.-O. Moch, Nucl. Phys. B 751 (2006) 18–52

Theoretical framework

Single-inclusive annihilation

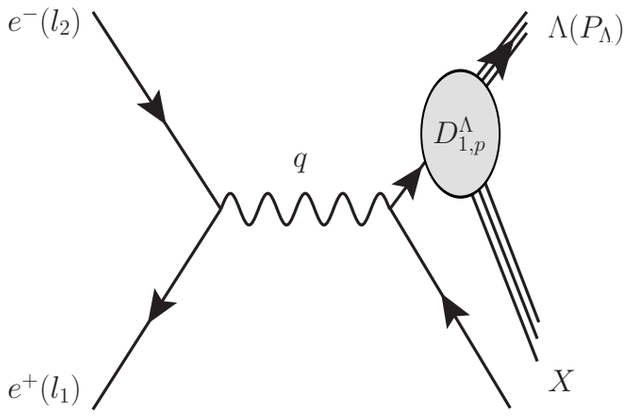

$$\frac{d\sigma^h}{dz} = \frac{4\pi\alpha^2(Q)}{Q^2} F_2^h(z,Q)$$

$$F_2^h(z,Q) = \frac{1}{n_f}\sum_q^{n_f} \hat{e}_q^2(Q)\Big[C_{2,q}^S\left(z,\alpha_s(Q)\right)\otimes D_{1,\Sigma}^h\left(z,Q\right) + C_{2,q}^{NS}\left(z,\alpha_s(Q)\right)\otimes D_{1,NS}^h\left(z,Q\right) + C_{2,g}^S\left(z,\alpha_s(Q)\right)\otimes D_{1,g}^h\left(z,Q\right)\Big]$$

P. J. Rijken and W. L. van Neerven, Phys. Lett. B 386 (1996) 422–428
P. J. Rijken and W. L. van Neerven, Nucl. Phys. B 487 (1997) 233–282
P. J. Rijken and W. L. van Neerven, Phys. Lett. B 392 (1997) 207–215
J. Blümlein and V. Ravindran, Nucl. Phys. B 749 (2006) 1–24
A. Mitov and S.-O. Moch, Nucl. Phys. B 751 (2006) 18–52

Charged-current semi-inclusive deep-inelastic scattering

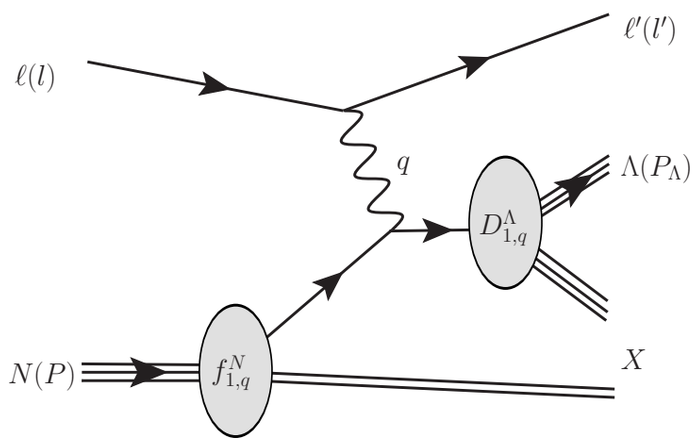

$$\frac{d^3\sigma}{dxdQdz} = \frac{4\pi\alpha^2}{xQ^3}\eta_W[Y_+F_T(x,z,Q) - 2(1-y)F_L(x,z,Q) + l_\ell Y\_xF_3(x,z,Q)]$$

$$Y_\pm = 1 \pm (1-y)^2 \qquad \eta_W = \frac{1}{2}\left(\frac{G_F M_W^2}{4\pi\alpha}\frac{Q^2}{Q^2+M_W^2}\right)^2$$

$$F_i^\Lambda(x,z,Q) = \sum_{p,p'} C_{pp'}(x,z,Q)\otimes f_{1,p}^N(x,Q)\otimes D_{1,p'}^\Lambda(z,Q) \quad i = L,T,3$$

L. Bonino et al., JHEP 10 (2025) 016
S. Goyal et al., Phys. Rev. D 111 (2025) 094007
S. Goyal et al., arXiv: 2603.30012

Theoretical framework

Single-inclusive annihilation

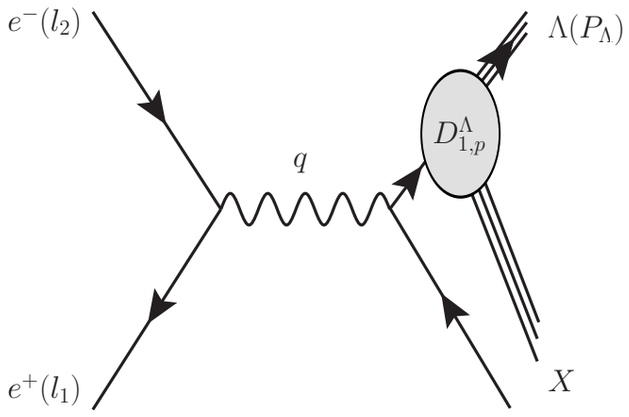

$$\frac{d\sigma^h}{dz} = \frac{4\pi\alpha^2(Q)}{Q^2} F_2^h(z,Q)$$

$$F_2^h(z,Q) = \frac{1}{n_f}\sum_q^{n_f} \hat{e}_q^2(Q)\Big[C_{2,q}^S\left(z,\alpha_s(Q)\right)\otimes D_{1,\Sigma}^h\left(z,Q\right) + C_{2,q}^{NS}\left(z,\alpha_s(Q)\right)\otimes D_{1,NS}^h\left(z,Q\right) + C_{2,g}^S\left(z,\alpha_s(Q)\right)\otimes D_{1,g}^h\left(z,Q\right)\Big]$$

P. J. Rijken and W. L. van Neerven, Phys. Lett. B 386 (1996) 422–428
P. J. Rijken and W. L. van Neerven, Nucl. Phys. B 487 (1997) 233–282
P. J. Rijken and W. L. van Neerven, Phys. Lett. B 392 (1997) 207–215
J. Blümlein and V. Ravindran, Nucl. Phys. B 749 (2006) 1–24
A. Mitov and S.-O. Moch, Nucl. Phys. B 751 (2006) 18–52

Charged-current semi-inclusive deep-inelastic scattering

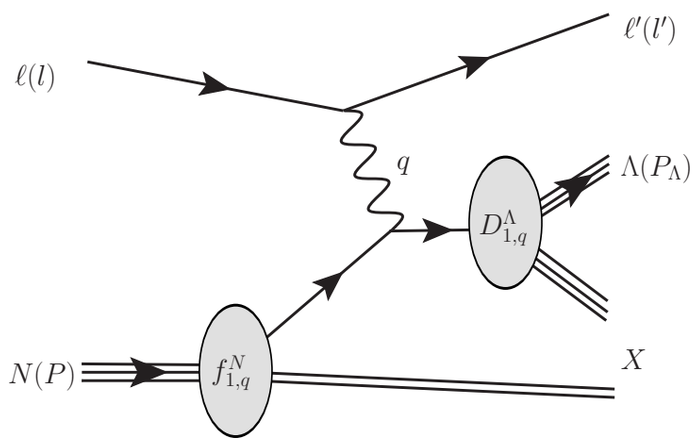

$$\frac{d^3\sigma}{dxdQdz} = \frac{4\pi\alpha^2}{xQ^3}\eta_W[Y_+F_T(x,z,Q) - 2(1-y)F_L(x,z,Q) + l_\ell Y\_xF_3(x,z,Q)]$$

$$Y_\pm = 1 \pm (1-y)^2 \qquad \eta_W = \frac{1}{2}\left(\frac{G_F M_W^2}{4\pi\alpha}\frac{Q^2}{Q^2+M_W^2}\right)^2$$

$$F_i^\Lambda(x,z,Q) = \sum_{p,p'} C_{pp'}(x,z,Q)\otimes f_{1,p}^N(x,Q)\otimes D_{1,p'}^\Lambda(z,Q) \quad i = L,T,3$$

L. Bonino et al., JHEP 10 (2025) 016
S. Goyal et al., Phys. Rev. D 111 (2025) 094007
S. Goyal et al., arXiv: 2603.30012

Coefficient functions and cross section computation handled by APFEL++ library [V. Bertone, arXiv: 1708.00911]
NNPDF31_nnlo_pch_as_0118 PDF set for SIDIS cross section
Heavy-quark mass effects treated within ZM-VFNS

Experimental data

Experiment	$\sqrt{s}$ [GeV]	$N_{\rm dat}^{\Lambda+\bar{\Lambda}}$
SIA		
ARGUS	10.0	16
Belle	10.52	15
TASSO14	14.0	3
TASSO22	22.0	4
TASSO33.3	33.3	5
TASSO34	34.0	7
TASSO34.8	34.8	10
TASSO42.1	42.1	4
CELLO	35.0	7
MARK II	29.0	13
HRS	29.0	12
SLD	91.2	15
	91.2	8
	91.2	8
	91.2	8
ALEPH	91.2	25
DELPHI91	91.2	10
OPAL	91.2	15

Experiment	$\sqrt{s}$ [GeV]	$N_{\rm dat}^{\Lambda} + N_{\rm dat}^{\bar{\Lambda}}$
Neutral-Current SIDIS		
CHIO	20.6	$3 + 4$
EMC	23.5	$4 + 3$
E665	30.3	$3 + 3$
H1 1996	300	2
ZEUS 10−40	319	1
ZEUS 40−160	319	2
ZEUS 160−640	319	4
ZEUS 640−2560	319	3
ZEUS 2560−10240	319	1
Charged-Current SIDIS		
WA59	9.2	$6 + 0$
NOMAD	9.3	$6 + 7$
ABCMO	23.5	$4 + 0$
Total		241

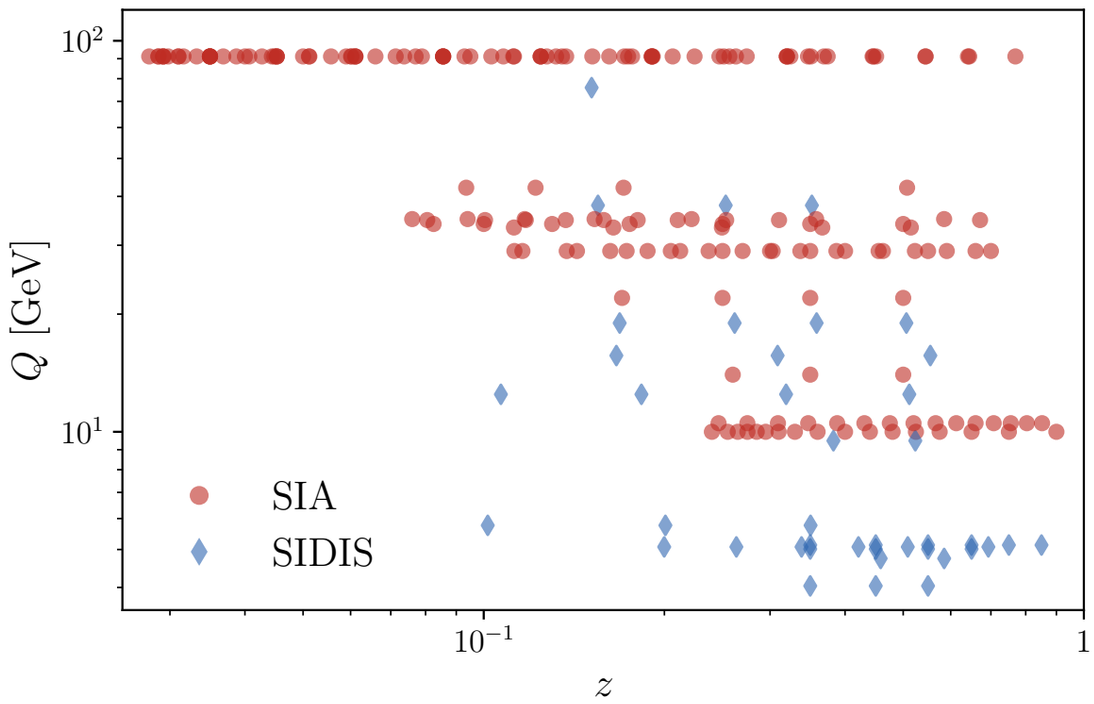

SIA Range in $\sqrt{s}$ spans from $10\,\mathrm{GeV}$ to M_Z

Datasets delivered as the sum of Λ and $\bar{\Lambda}$

SIDIS Measurements for neutral- and charged-current

Data provided separately for Λ and $\bar{\Lambda}$

Constraints and kinematics

Measurements differential in other variables handled by computing differential cross sections multiplied by a Jacobian factor that includes **hadron mass corrections**

Constraints and kinematics

Measurements differential in other variables handled by computing differential cross sections multiplied by a Jacobian factor that includes **hadron mass corrections**

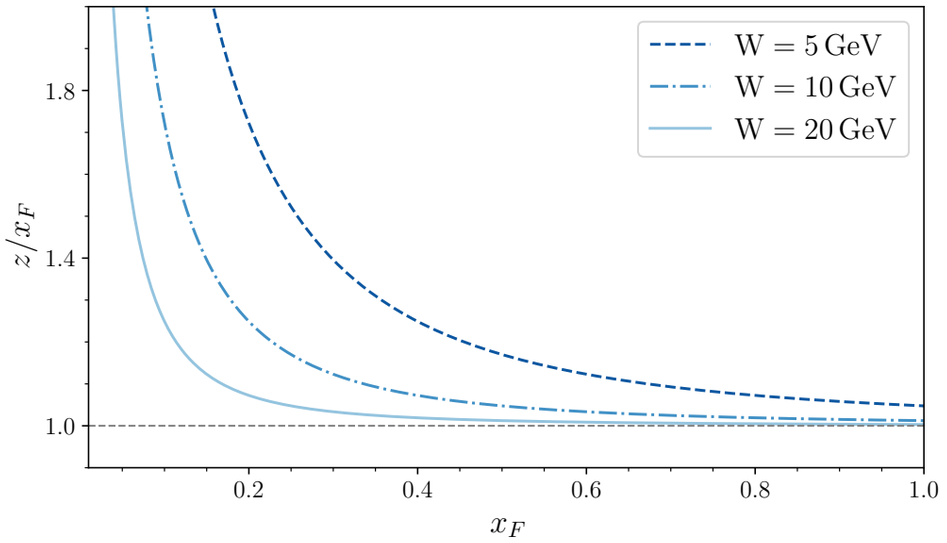

- For SIA, in terms of $x_p = \dfrac{2p_\Lambda}{\sqrt{s}}$

$$z(x_p, M_\Lambda) = x_p \sqrt{1 + \frac{4M_\Lambda^2}{x_p^2 s}}$$

Albino, et al. Nucl. Phys. B 803 (2008),
NNPDF Collaboration, Eur. Phys. J. C 77 (2017) 516

- For SIDIS, in terms of $x_F = \dfrac{2p_{\Lambda,L}}{W}$

$$z(x_F, M_\Lambda) \simeq \frac{x_F}{2}\left(1 + \sqrt{1 + \frac{4M_\Lambda^2}{x_F^2 W^2}}\right)$$

restricting to $x_F > 0$ for hadrons produced in the *current fragmentation region*

Constraints and kinematics

Measurements differential in other variables handled by computing differential cross sections multiplied by a Jacobian factor that includes **hadron mass corrections**

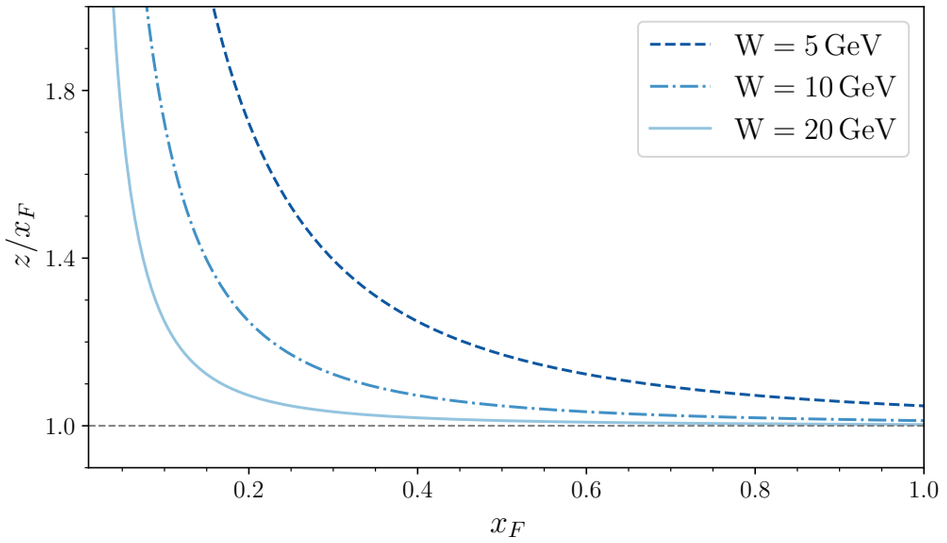

- For SIA, in terms of $x_p = \dfrac{2p_\Lambda}{\sqrt{s}}$

$$z(x_p, M_\Lambda) = x_p \sqrt{1 + \frac{4M_\Lambda^2}{x_p^2 s}}$$

Albino, et al. Nucl. Phys. B 803 (2008),
NNPDF Collaboration, Eur. Phys. J. C 77 (2017) 516

- For SIDIS, in terms of $x_F = \dfrac{2p_{\Lambda,L}}{W}$

$$z(x_F, M_\Lambda) \simeq \frac{x_F}{2}\left(1 + \sqrt{1 + \frac{4M_\Lambda^2}{x_F^2 W^2}}\right)$$

restricting to $x_F > 0$ for hadrons produced in the *current fragmentation region*

Integration of numerator and denominator for multiplicities separately over the accepted phase space (y ranges and $W_{\min}$ given by the single experiments) taking into account our selection criteria

Constraints and kinematics

Measurements differential in other variables handled by computing differential cross sections multiplied by a Jacobian factor that includes **hadron mass corrections**

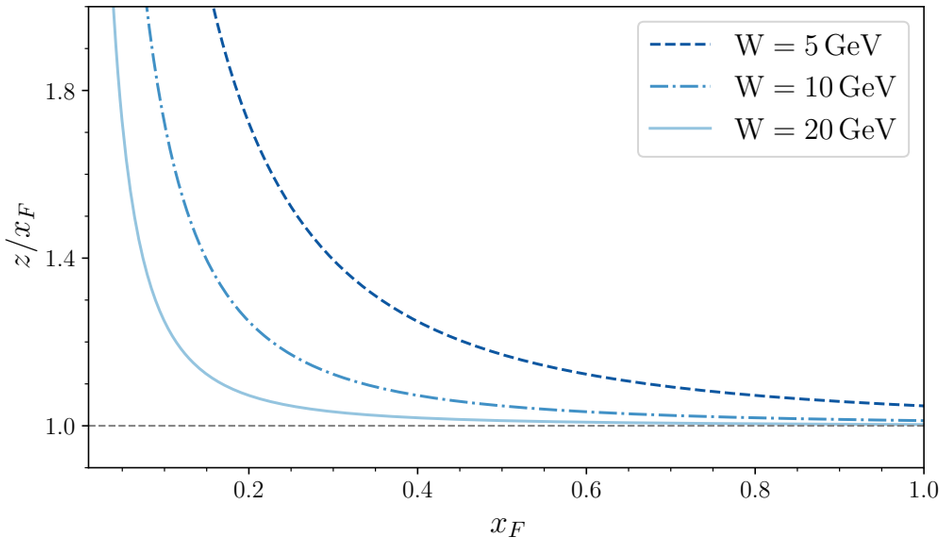

- For SIA, in terms of $x_p = \dfrac{2p_\Lambda}{\sqrt{s}}$

$$z(x_p, M_\Lambda) = x_p \sqrt{1 + \frac{4M_\Lambda^2}{x_p^2 s}}$$

Albino, et al. Nucl. Phys. B 803 (2008),
NNPDF Collaboration, Eur. Phys. J. C 77 (2017) 516

- For SIDIS, in terms of $x_F = \dfrac{2p_{\Lambda,L}}{W}$

$$z(x_F, M_\Lambda) \simeq \frac{x_F}{2}\left(1 + \sqrt{1 + \frac{4M_\Lambda^2}{x_F^2 W^2}}\right)$$

restricting to $x_F > 0$ for hadrons produced in the *current fragmentation region*

Integration of numerator and denominator for multiplicities separately over the accepted phase space (y ranges and $W_{\min}$ given by the single experiments) taking into account our selection criteria

$$\frac{1}{\sigma_{\rm DIS}}\frac{d\sigma}{dz} = \frac{\int_{z_{\min}}^{z_{\max}} dz \int_{Q_{\min}}^{Q_{\max}} dQ \int_{x_{\min}}^{x_{\max}} dx \frac{d^3\sigma}{dx dQ dz}}{\Delta z \int_{Q_{\min}}^{Q_{\max}} dQ \int_{x_{\min}}^{x_{\max}} dx \frac{d^2\sigma_{\rm DIS}}{dx dQ}}$$

Constraints and kinematics

Measurements differential in other variables handled by computing differential cross sections multiplied by a Jacobian factor that includes **hadron mass corrections**

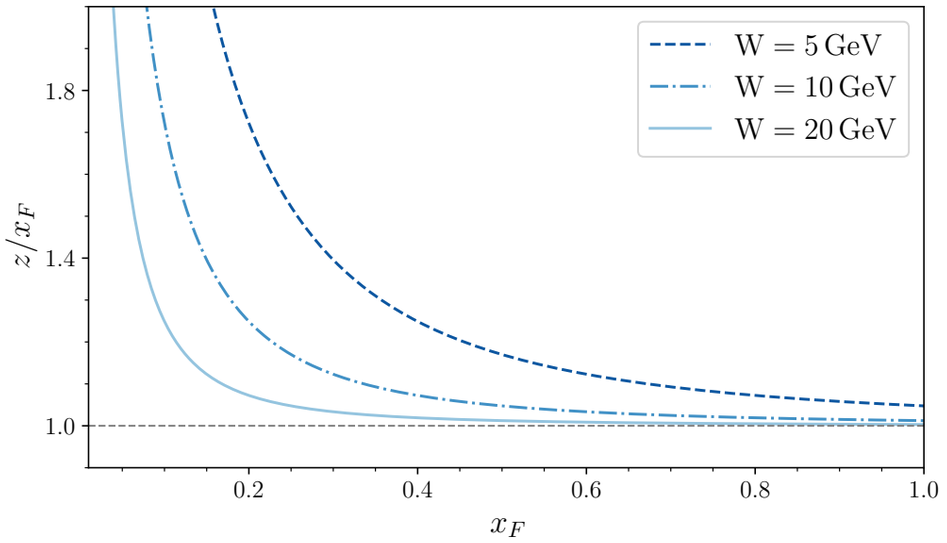

- For SIA, in terms of $x_p = \dfrac{2p_\Lambda}{\sqrt{s}}$

$$z(x_p, M_\Lambda) = x_p \sqrt{1 + \frac{4M_\Lambda^2}{x_p^2 s}}$$

Albino, et al. Nucl. Phys. B 803 (2008),
NNPDF Collaboration, Eur. Phys. J. C 77 (2017) 516

- For SIDIS, in terms of $x_F = \dfrac{2p_{\Lambda,L}}{W}$

$$z(x_F, M_\Lambda) \simeq \frac{x_F}{2}\left(1 + \sqrt{1 + \frac{4M_\Lambda^2}{x_F^2 W^2}}\right)$$

restricting to $x_F > 0$ for hadrons produced in the *current fragmentation region*

Integration of numerator and denominator for multiplicities separately over the accepted phase space (y ranges and $W_{\min}$ given by the single experiments) taking into account our selection criteria

$$\frac{1}{\sigma_{\rm DIS}}\frac{d\sigma}{dz} = \frac{\int_{z_{\min}}^{z_{\max}} dz \int_{Q_{\min}}^{Q_{\max}} dQ \int_{x_{\min}}^{x_{\max}} dx \frac{d^3\sigma}{dx dQ dz}}{\Delta z \int_{Q_{\min}}^{Q_{\max}} dQ \int_{x_{\min}}^{x_{\max}} dx \frac{d^2\sigma_{\rm DIS}}{dx dQ}}$$

If no Q_{max} is provided, $Q_{min} \leq Q \leq y_{max}\sqrt{s}$

Process		Q range	z range
SIA	$\sqrt{s} < M_Z$	$Q = \sqrt{s}$	$0.075 < z < 0.9$
	$\sqrt{s} = M_Z$		$0.02 < z < 0.9$
SIDIS	Λ , $\frac{d\sigma}{dz}$	$Q \geq 1$ GeV	$0.3 < z < 0.9$
	$\bar{\Lambda}$, $\frac{d\sigma}{dz}$		$0.2 < z < 0.9$
	$\frac{d\sigma}{dx_F}$		$0.1 < z < 0.9$

Fit Methodology

The adopted statistical framework relies on Monte Carlo sampling method, which propagates experimental uncertainties in the parameters of the FFs.

The FF set consists of $N_{\rm rep} = 100$ replicas.

FFs parametrised in terms of a **one-layered feed-forward neural network** $\mathcal{N}_i(z,\theta)$ at the initial scale of $\mu_0 = 5\,\mathrm{GeV}$

$$z\,D^{\Lambda}_{1,i}(z,\mu_0 = 5\,\mathrm{GeV}) = \mathcal{N}_{\rm i}(\mathrm{z},\theta) - \mathcal{N}_{\rm i}(1,\theta)$$

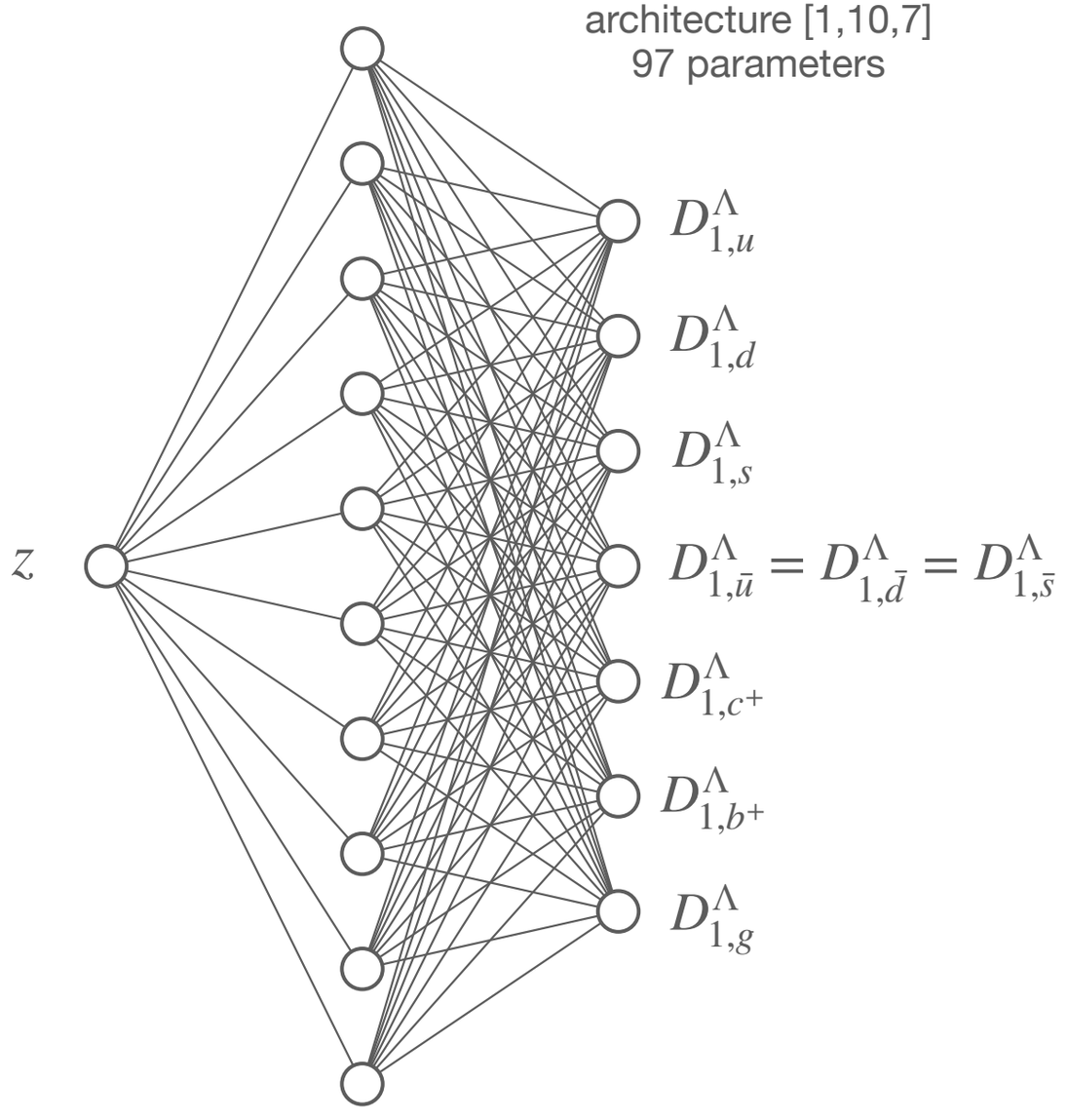

Fit Methodology

The adopted statistical framework relies on Monte Carlo sampling method, which propagates experimental uncertainties in the parameters of the FFs.

The FF set consists of $N_{\rm rep} = 100$ replicas.

FFs parametrised in terms of a **one-layered feed-forward neural network** $\mathcal{N}_i(z,\theta)$ at the initial scale of $\mu_0 = 5\,\mathrm{GeV}$

$$z\,D_{1,i}^{\Lambda}(z,\mu_0 = 5\,\mathrm{GeV}) = \mathcal{N}_{\rm i}(\mathrm{z},\theta) - \mathcal{N}_{\rm i}(1,\theta)$$

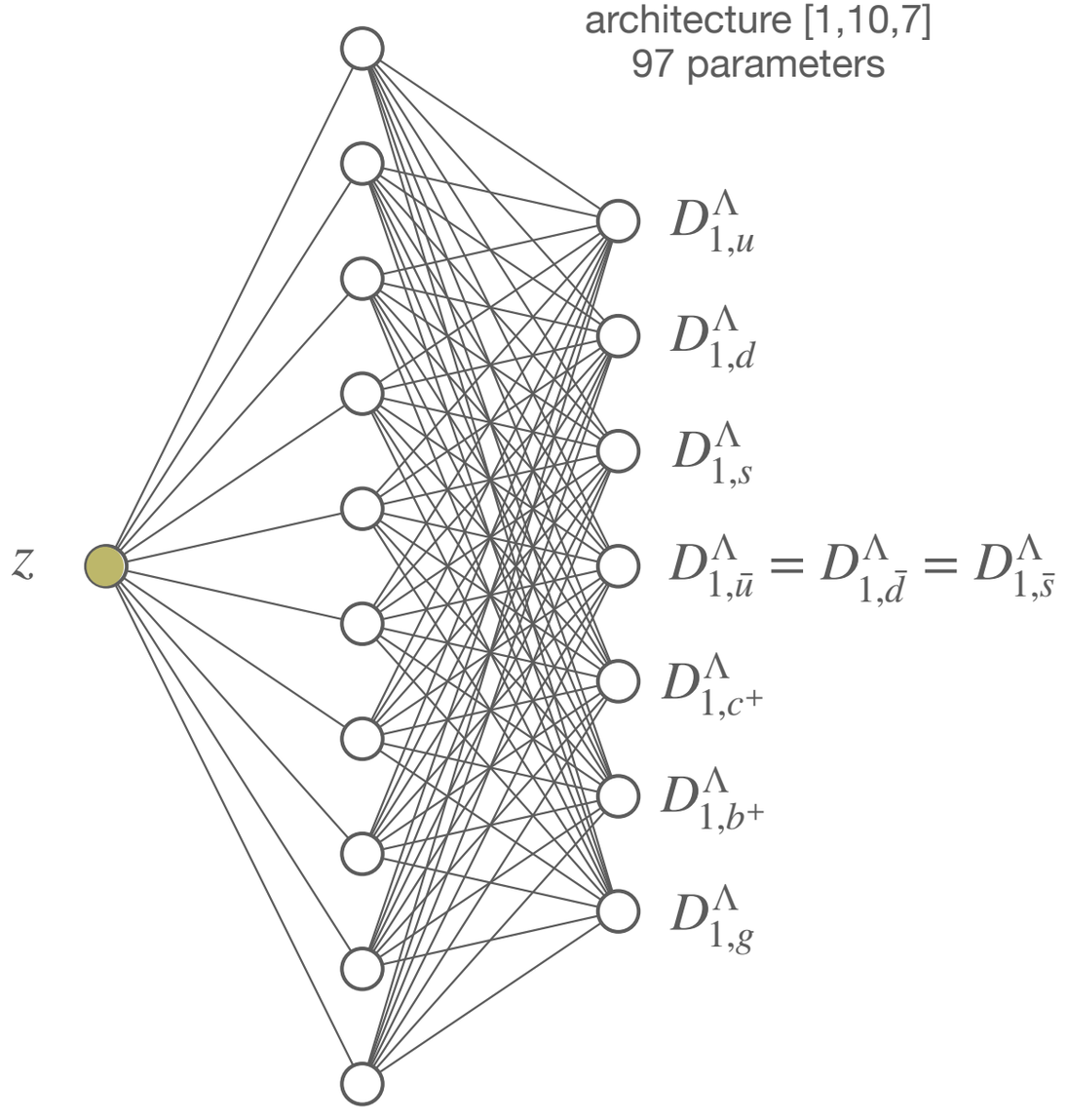

Fit Methodology

The adopted statistical framework relies on Monte Carlo sampling method, which propagates experimental uncertainties in the parameters of the FFs.

The FF set consists of $N_{\rm rep} = 100$ replicas.

FFs parametrised in terms of a **one-layered feed-forward neural network** $\mathcal{N}_i(z,\theta)$ at the initial scale of $\mu_0 = 5\,\mathrm{GeV}$

$$z\,D_{1,i}^{\Lambda}(z,\mu_0 = 5\,\mathrm{GeV}) = \mathcal{N}_{\rm i}(\mathrm{z},\theta) - \mathcal{N}_{\rm i}(1,\theta)$$

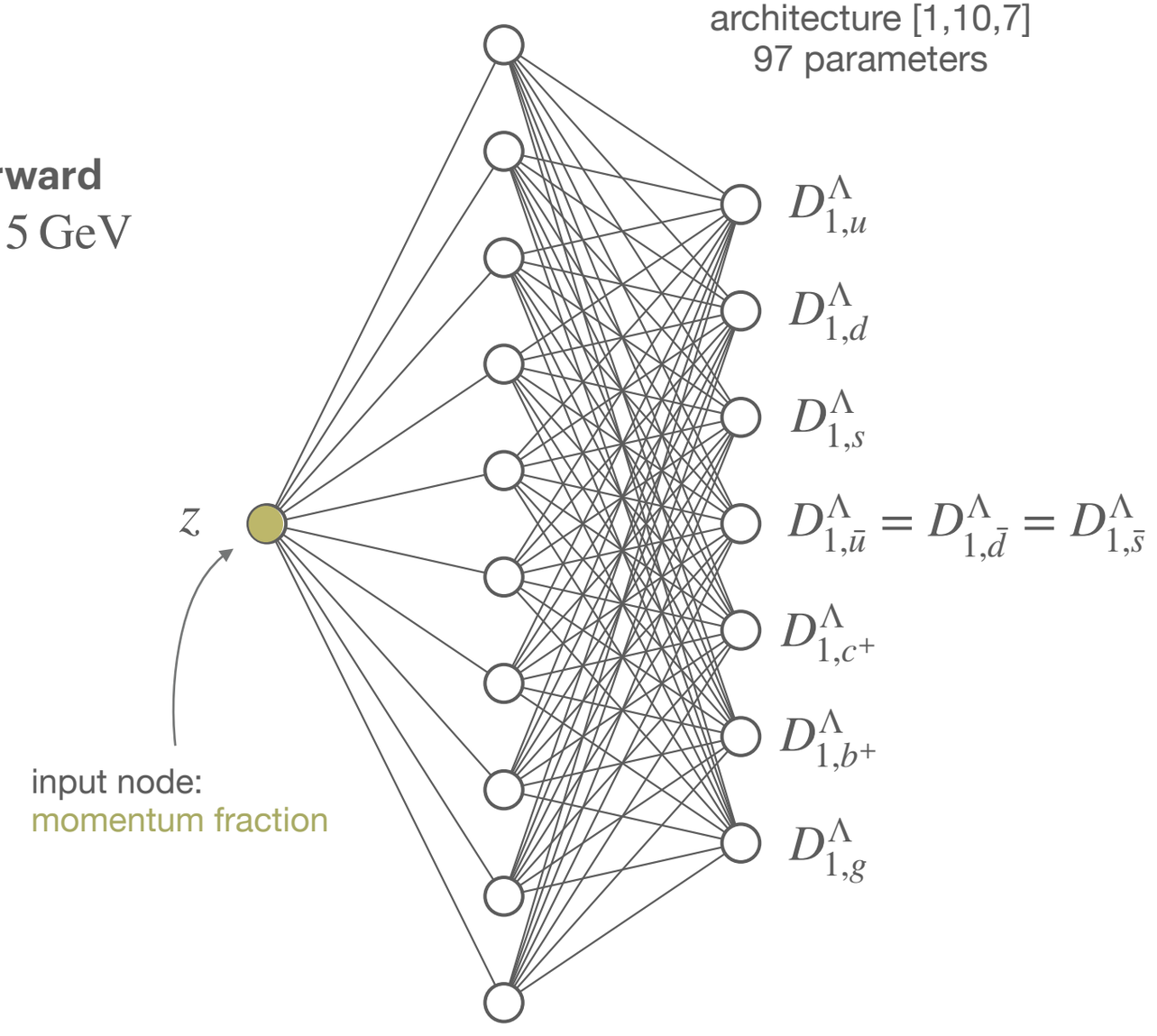

Fit Methodology

The adopted statistical framework relies on Monte Carlo sampling method, which propagates experimental uncertainties in the parameters of the FFs.

The FF set consists of $N_{\rm rep} = 100$ replicas.

FFs parametrised in terms of a **one-layered feed-forward neural network** $\mathcal{N}_i(z,\theta)$ at the initial scale of $\mu_0 = 5\,\mathrm{GeV}$

$$z\,D_{1,i}^{\Lambda}(z,\mu_0 = 5\,\mathrm{GeV}) = \mathcal{N}_{\rm i}(\mathrm{z},\theta) - \mathcal{N}_{\rm i}(1,\theta)$$

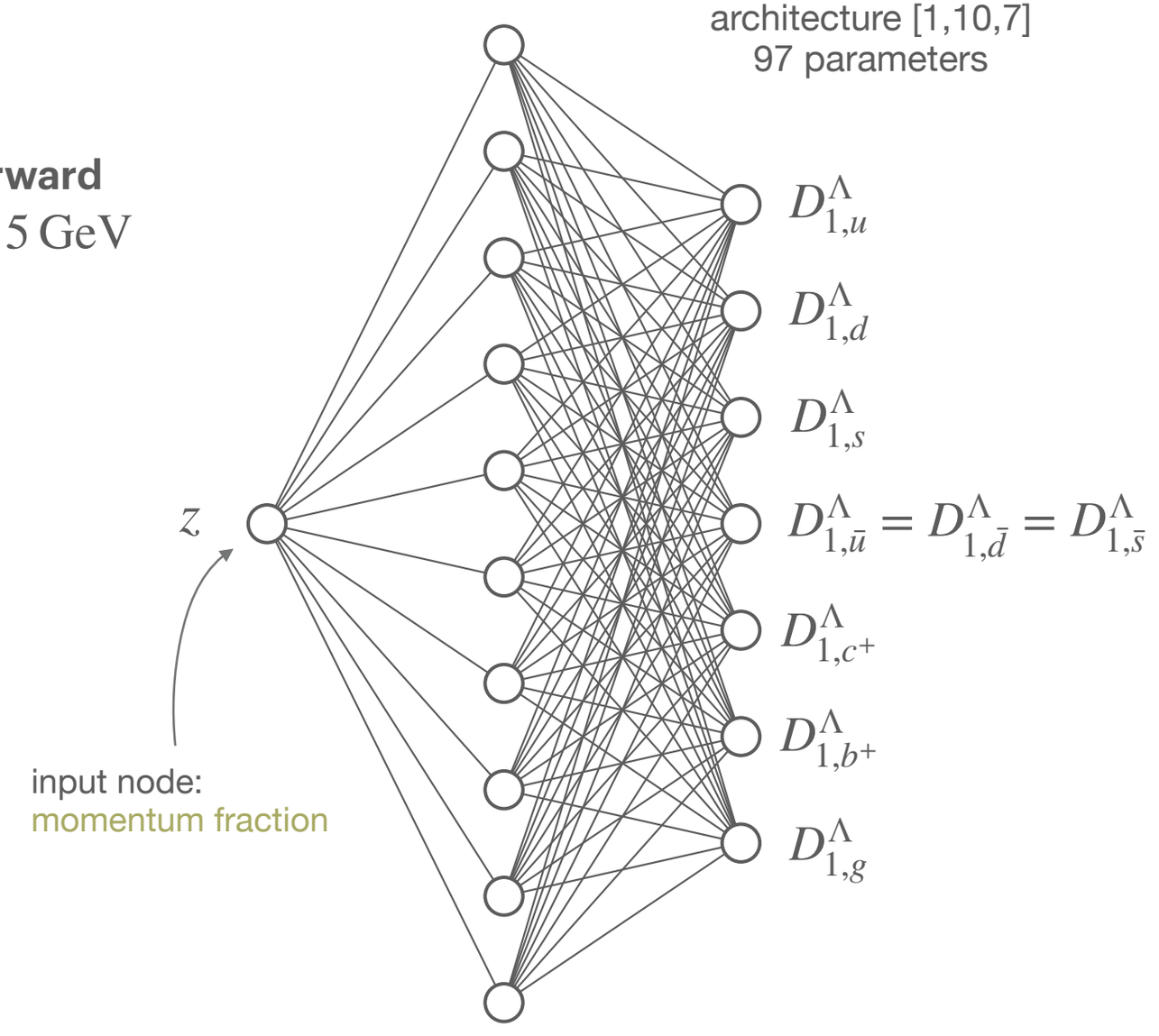

Fit Methodology

The adopted statistical framework relies on Monte Carlo sampling method, which propagates experimental uncertainties in the parameters of the FFs.

The FF set consists of $N_{\text{rep}} = 100$ replicas.

FFs parametrised in terms of a **one-layered feed-forward neural network** $\mathcal{N}_i(z,\theta)$ at the initial scale of $\mu_0 = 5\,\text{GeV}$

$$z\,D_{1,i}^{\Lambda}(z,\mu_0 = 5\,\text{GeV}) = \mathcal{N}_{\text{i}}(\text{z},\theta) - \mathcal{N}_{\text{i}}(1,\theta)$$

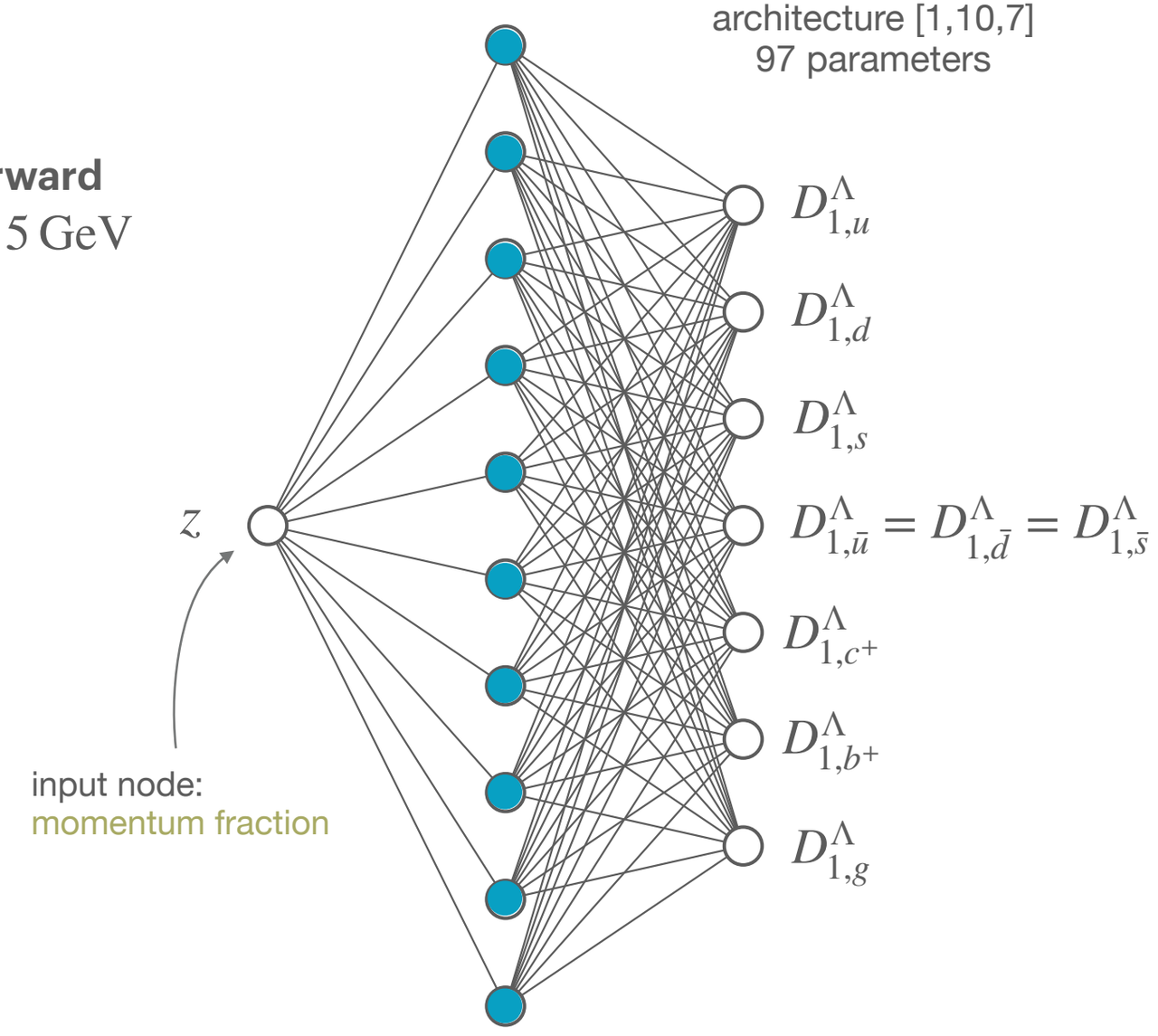

Fit Methodology

The adopted statistical framework relies on Monte Carlo sampling method, which propagates experimental uncertainties in the parameters of the FFs.

The FF set consists of $N_{\text{rep}} = 100$ replicas.

FFs parametrised in terms of a **one-layered feed-forward neural network** $\mathcal{N}_i(z,\theta)$ at the initial scale of $\mu_0 = 5\,\text{GeV}$

$$z\,D_{1,i}^{\Lambda}(z,\mu_0 = 5\,\text{GeV}) = \mathcal{N}_{\text{i}}(\text{z},\theta) - \mathcal{N}_{\text{i}}(1,\theta)$$

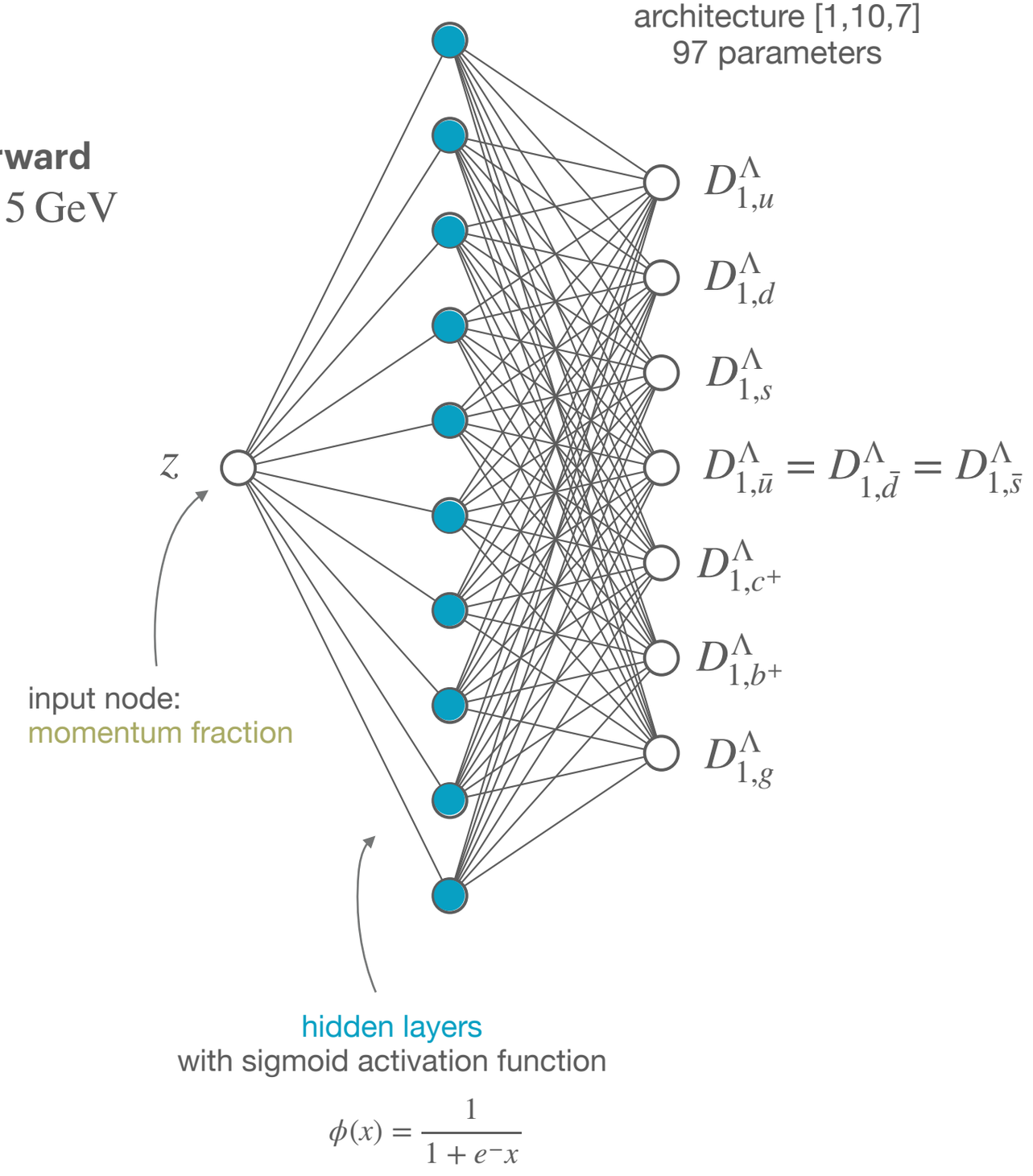

Fit Methodology

The adopted statistical framework relies on Monte Carlo sampling method, which propagates experimental uncertainties in the parameters of the FFs.

The FF set consists of $N_{\rm rep} = 100$ replicas.

FFs parametrised in terms of a **one-layered feed-forward neural network** $\mathcal{N}_i(z,\theta)$ at the initial scale of $\mu_0 = 5\,\mathrm{GeV}$

$$z\,D_{1,i}^{\Lambda}(z,\mu_0 = 5\,\mathrm{GeV}) = \mathcal{N}_{\rm i}(\mathrm{z},\theta) - \mathcal{N}_{\rm i}(1,\theta)$$

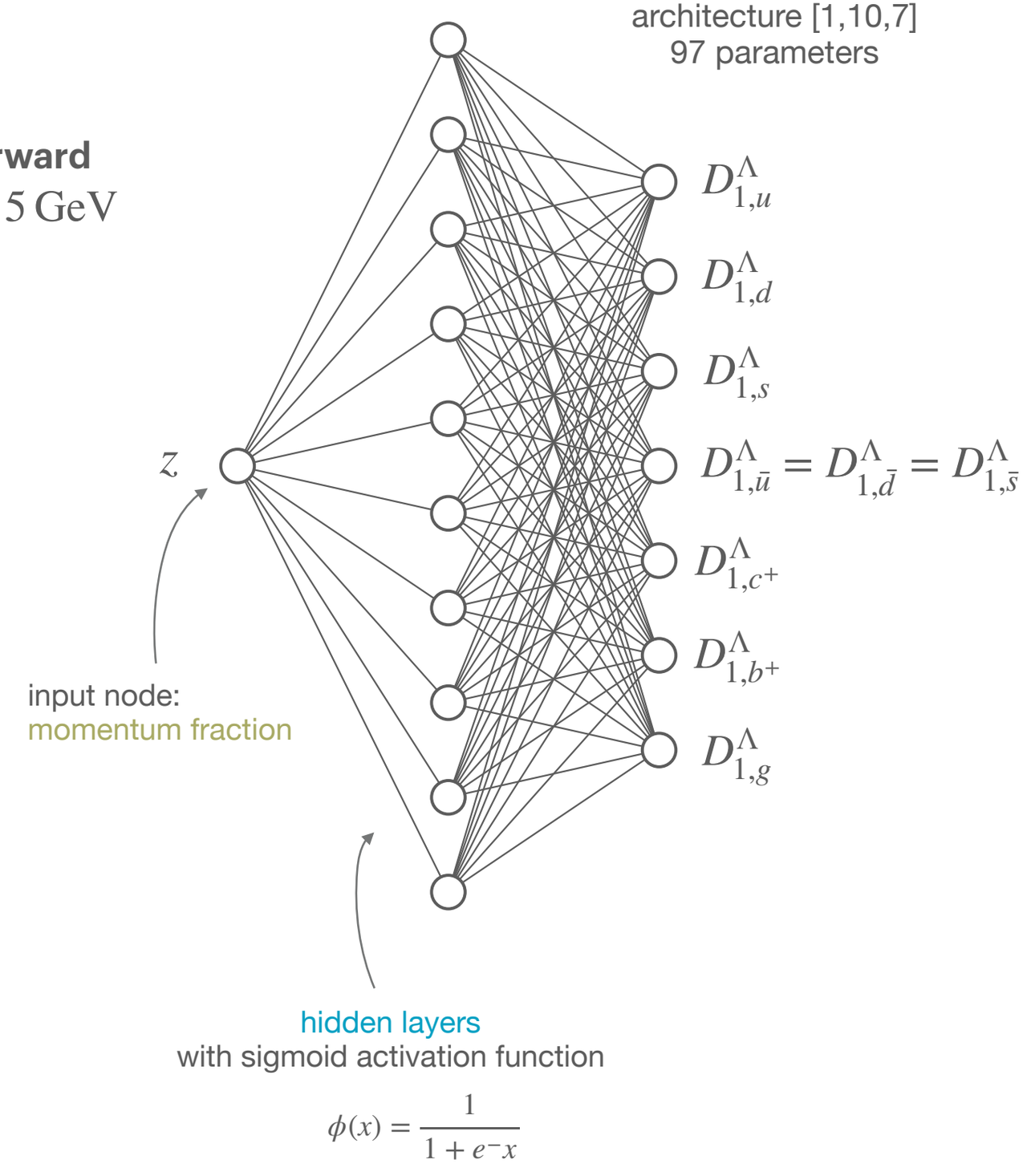

Fit Methodology

The adopted statistical framework relies on Monte Carlo sampling method, which propagates experimental uncertainties in the parameters of the FFs.

The FF set consists of $N_{\rm rep} = 100$ replicas.

FFs parametrised in terms of a **one-layered feed-forward neural network** $\mathcal{N}_i(z,\theta)$ at the initial scale of $\mu_0 = 5\,\mathrm{GeV}$

$$z\,D_{1,i}^{\Lambda}(z,\mu_0 = 5\,\mathrm{GeV}) = \mathcal{N}_{\rm i}(\mathrm{z},\theta) - \mathcal{N}_{\rm i}(1,\theta)$$

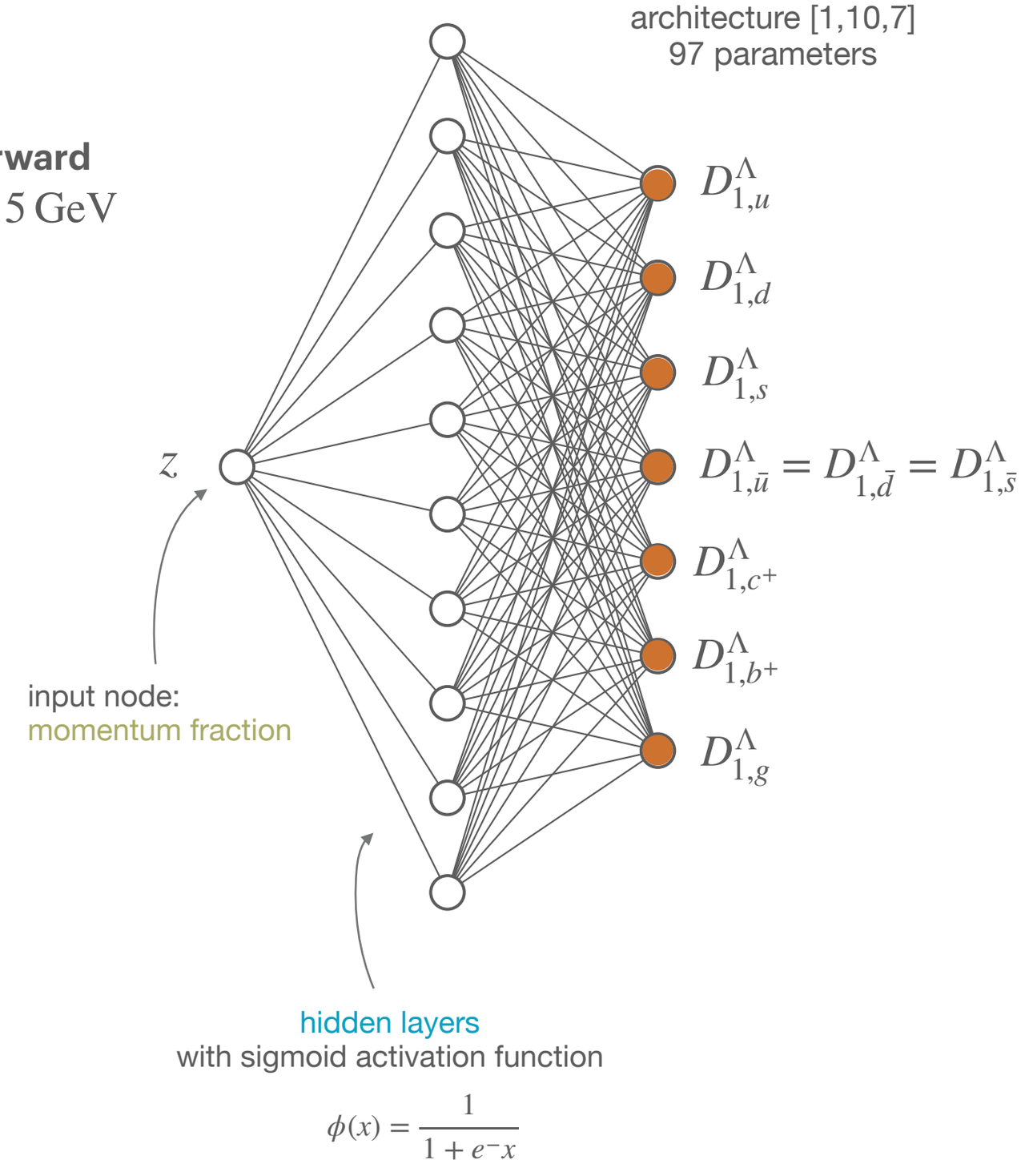

Fit Methodology

The adopted statistical framework relies on Monte Carlo sampling method, which propagates experimental uncertainties in the parameters of the FFs.

The FF set consists of $N_{\rm rep} = 100$ replicas.

FFs parametrised in terms of a **one-layered feed-forward neural network** $\mathcal{N}_i(z,\theta)$ at the initial scale of $\mu_0 = 5\,\mathrm{GeV}$

$$z\,D_{1,i}^{\Lambda}(z,\mu_0 = 5\,\mathrm{GeV}) = \mathcal{N}_{\rm i}(\mathrm{z},\theta) - \mathcal{N}_{\rm i}(1,\theta)$$

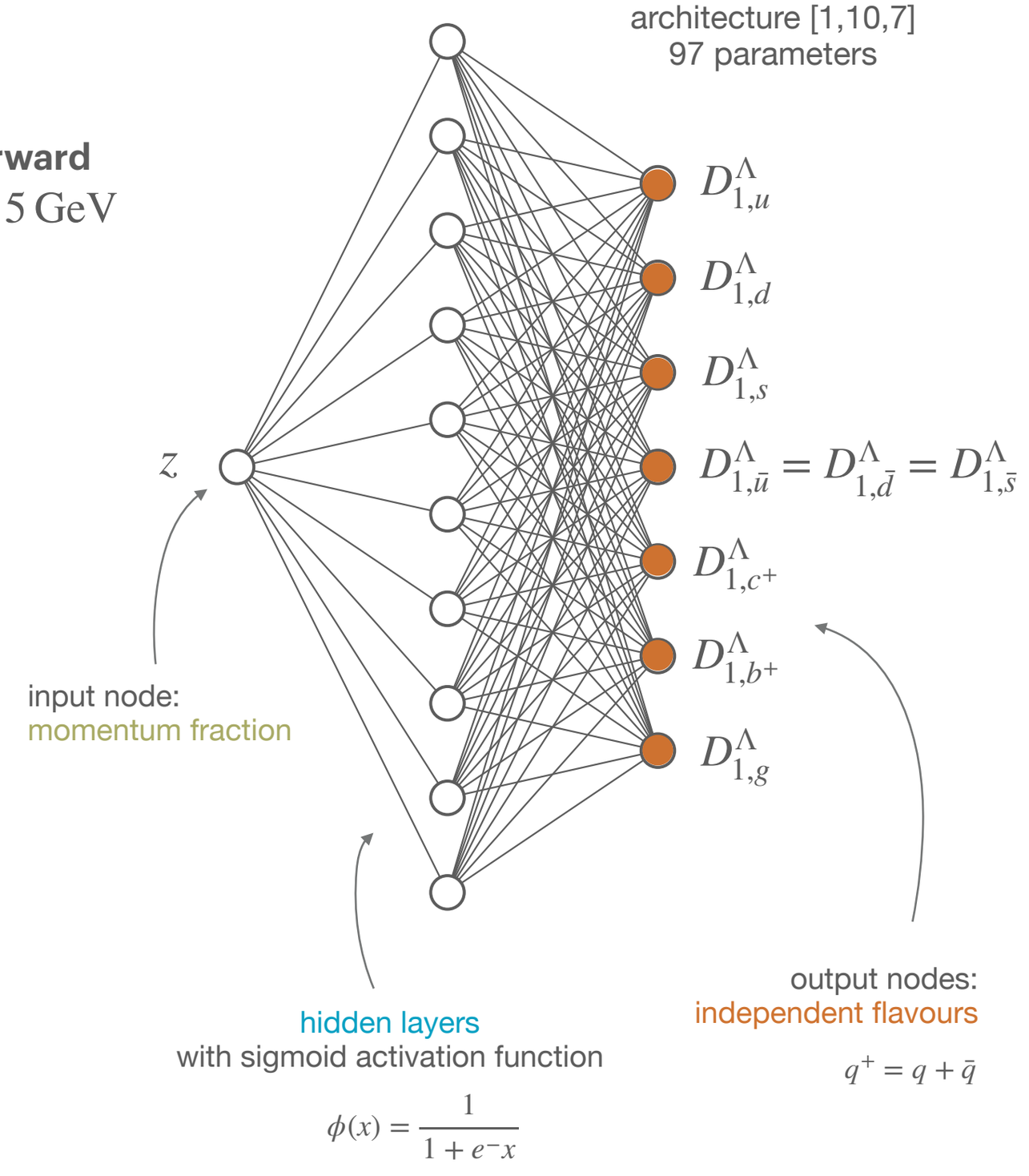

Fit Methodology

The adopted statistical framework relies on Monte Carlo sampling method, which propagates experimental uncertainties in the parameters of the FFs.

The FF set consists of $N_{\rm rep} = 100$ replicas.

FFs parametrised in terms of a **one-layered feed-forward neural network** $\mathcal{N}_i(z,\theta)$ at the initial scale of $\mu_0 = 5\,\mathrm{GeV}$

$$z\,D_{1,i}^{\Lambda}(z,\mu_0 = 5\,\mathrm{GeV}) = \mathcal{N}_{\rm i}(\mathrm{z},\theta) - \mathcal{N}_{\rm i}(1,\theta)$$

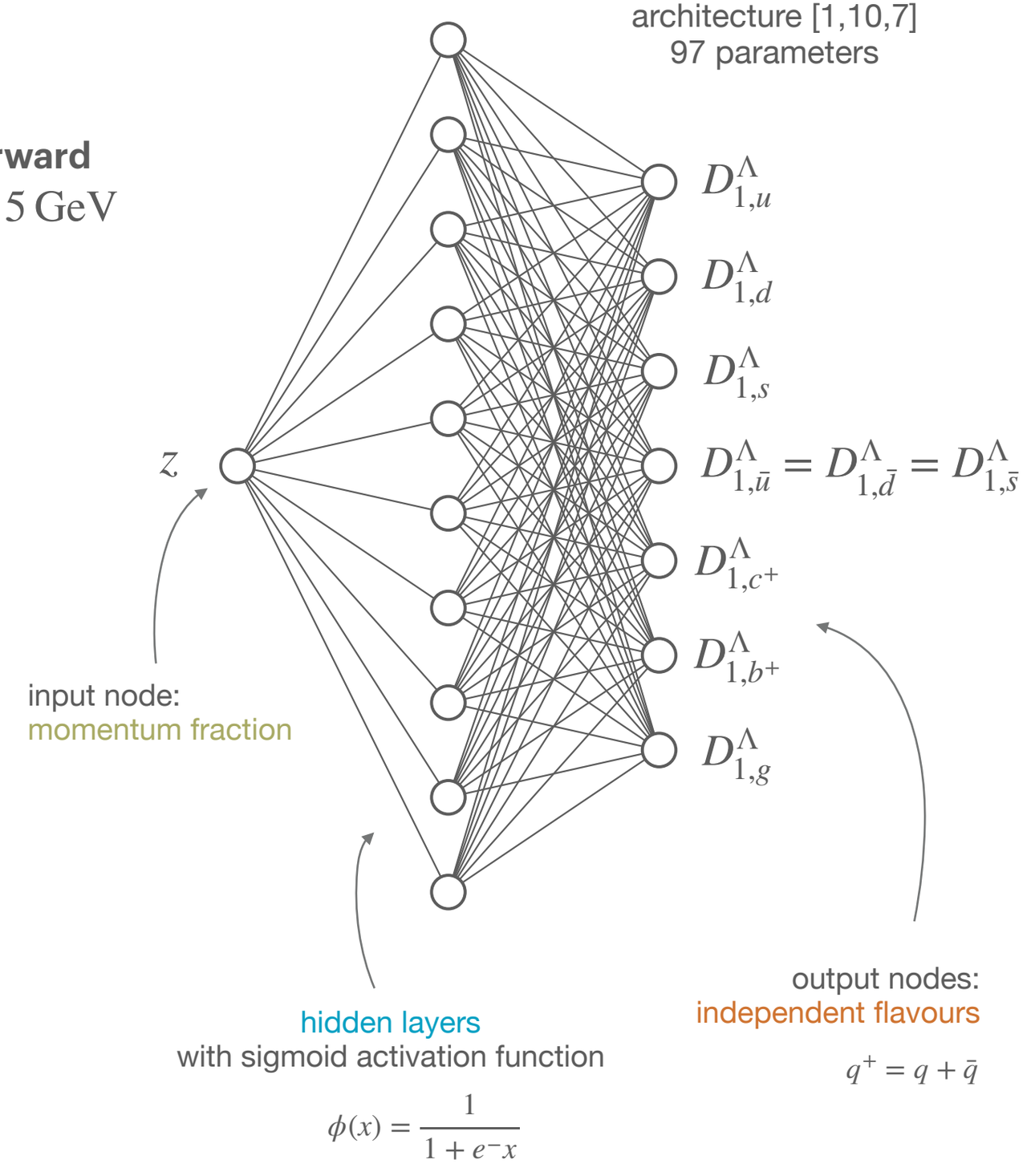

Fit Methodology

The adopted statistical framework relies on Monte Carlo sampling method, which propagates experimental uncertainties in the parameters of the FFs.

The FF set consists of $N_{\text{rep}} = 100$ replicas.

FFs parametrised in terms of a **one-layered feed-forward neural network** $\mathcal{N}_i(z,\theta)$ at the initial scale of $\mu_0 = 5\,\text{GeV}$

$$z\,D_{1,i}^{\Lambda}(z,\mu_0 = 5\,\text{GeV}) = \mathcal{N}_{\text{i}}(\text{z},\theta) - \mathcal{N}_{\text{i}}(1,\theta)$$

Analytic computation by NNAD library [2005.07039]

Cross-validation with training fraction of 50% to avoid overfitting

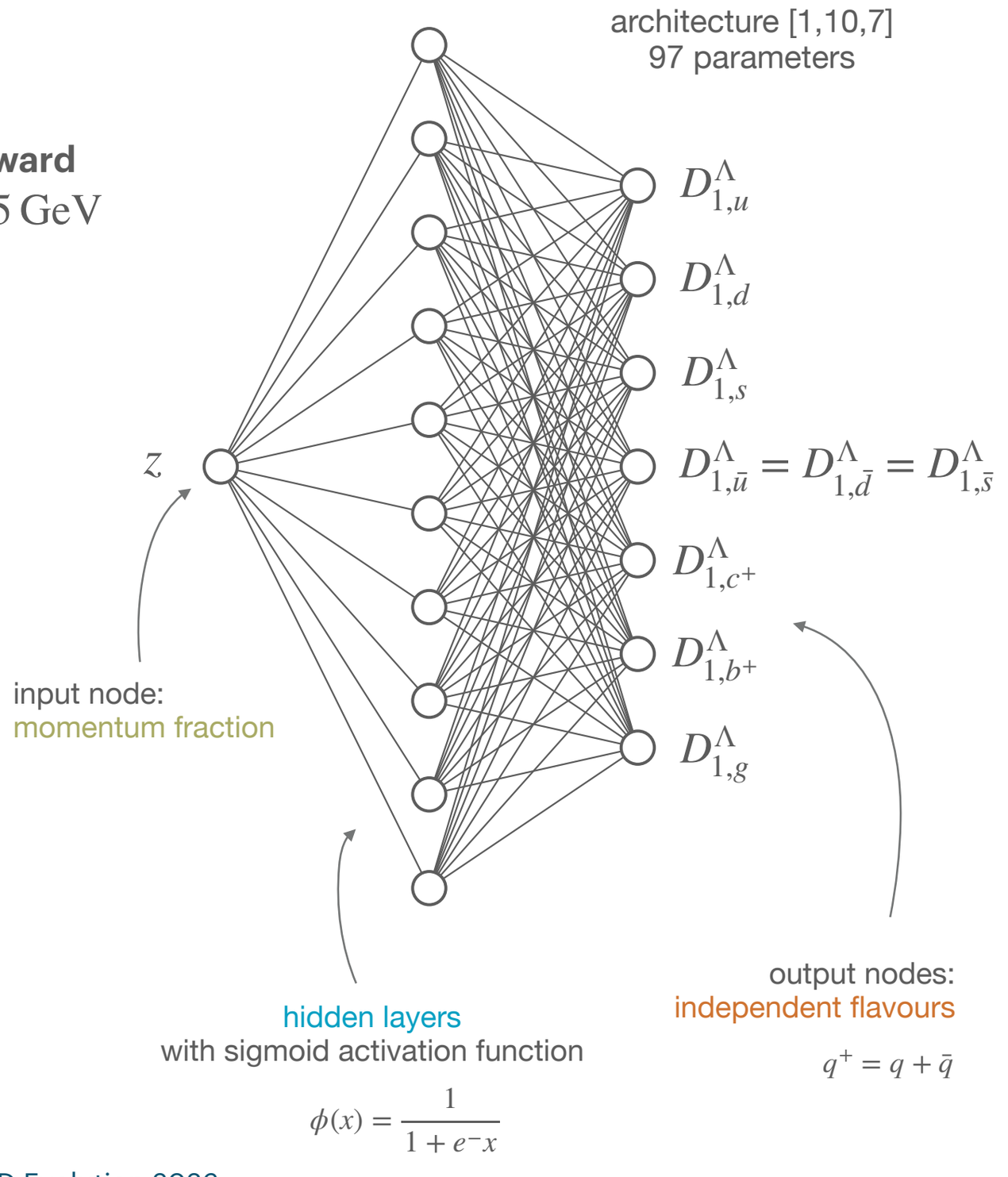

Fit Methodology

The adopted statistical framework relies on Monte Carlo sampling method, which propagates experimental uncertainties in the parameters of the FFs.

The FF set consists of $N_{\text{rep}} = 100$ replicas.

FFs parametrised in terms of a **one-layered feed-forward neural network** $\mathcal{N}_i(z,\theta)$ at the initial scale of $\mu_0 = 5\,\text{GeV}$

$$z\,D_{1,i}^{\Lambda}(z,\mu_0 = 5\,\text{GeV}) = \mathcal{N}_{\text{i}}(\text{z},\theta) - \mathcal{N}_{\text{i}}(1,\theta)$$

Analytic computation by NNAD library [2005.07039]

Cross-validation with training fraction of 50% to avoid overfitting

Levenberg-Marquardt algorithm for **minimisation** implemented in Ceres Solver

$$\chi^{2(k)} \equiv \left(T(\theta^{(k)}) - x^{(k)}\right)^T C^{-1} \left(T(\theta^{(k)}) - x^{(k)}\right)$$

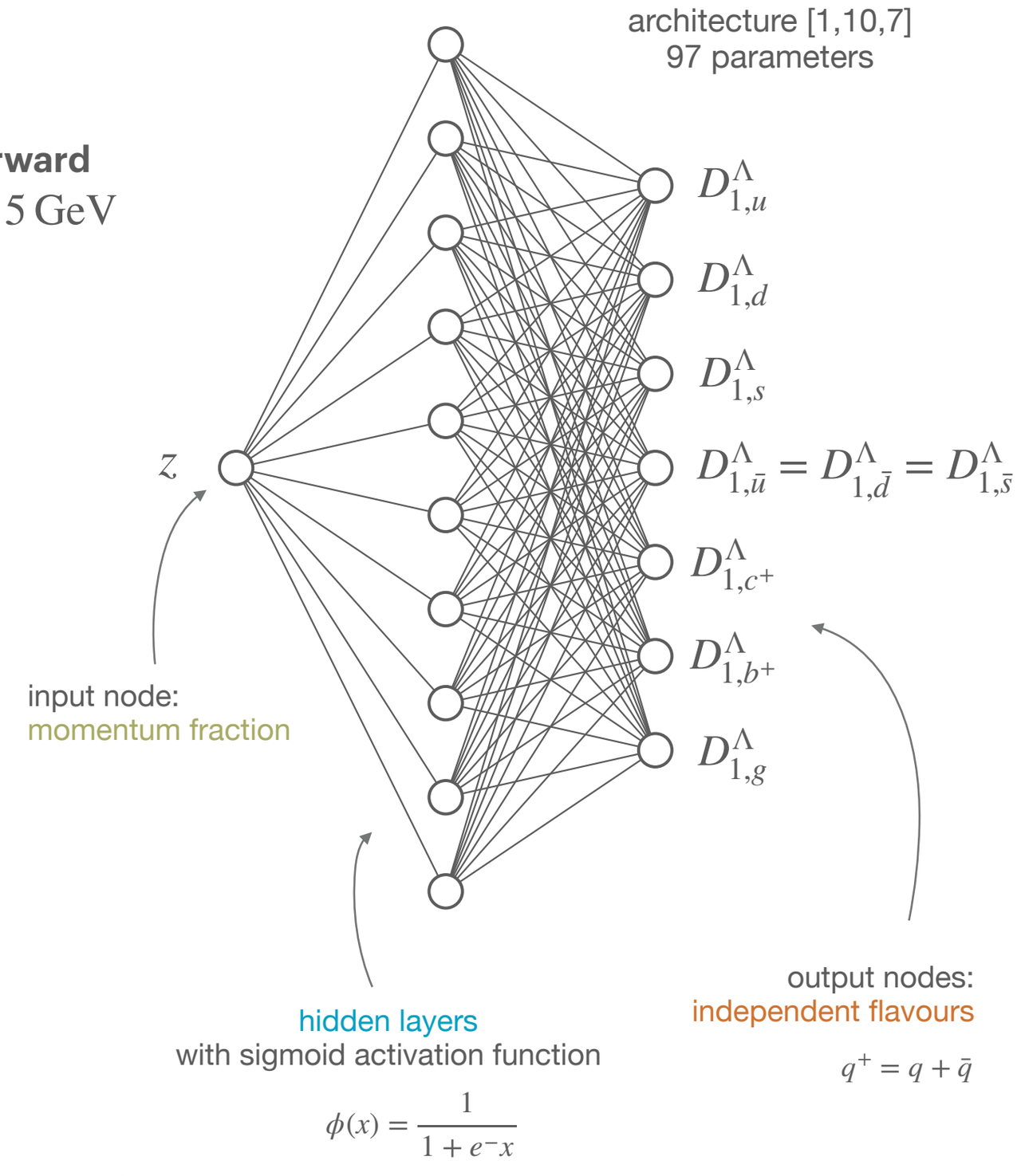

Fit Methodology

The adopted statistical framework relies on Monte Carlo sampling method, which propagates experimental uncertainties in the parameters of the FFs.

The FF set consists of $N_{\text{rep}} = 100$ replicas.

FFs parametrised in terms of a **one-layered feed-forward neural network** $\mathcal{N}_i(z,\theta)$ at the initial scale of $\mu_0 = 5\,\text{GeV}$

$$z\,D_{1,i}^{\Lambda}(z,\mu_0 = 5\,\text{GeV}) = \mathcal{N}_{\text{i}}(\text{z},\theta) - \mathcal{N}_{\text{i}}(1,\theta)$$

Analytic computation by NNAD library [2005.07039]

Cross-validation with training fraction of 50% to avoid overfitting

Levenberg-Marquardt algorithm for **minimisation** implemented in Ceres Solver

$$\chi^{2(k)} \equiv \left(T(\theta^{(k)}) - x^{(k)}\right)^T C^{-1} \left(T(\theta^{(k)}) - x^{(k)}\right)$$

Alternative parameterisation: positivity requirement

$$z\,D_{1,i}^{\Lambda}(z,\mu_0 = 5\,\text{GeV}) = (\mathcal{N}_{\text{i}}(\text{z},\theta) - \mathcal{N}_{\text{i}}(1,\theta))^2$$

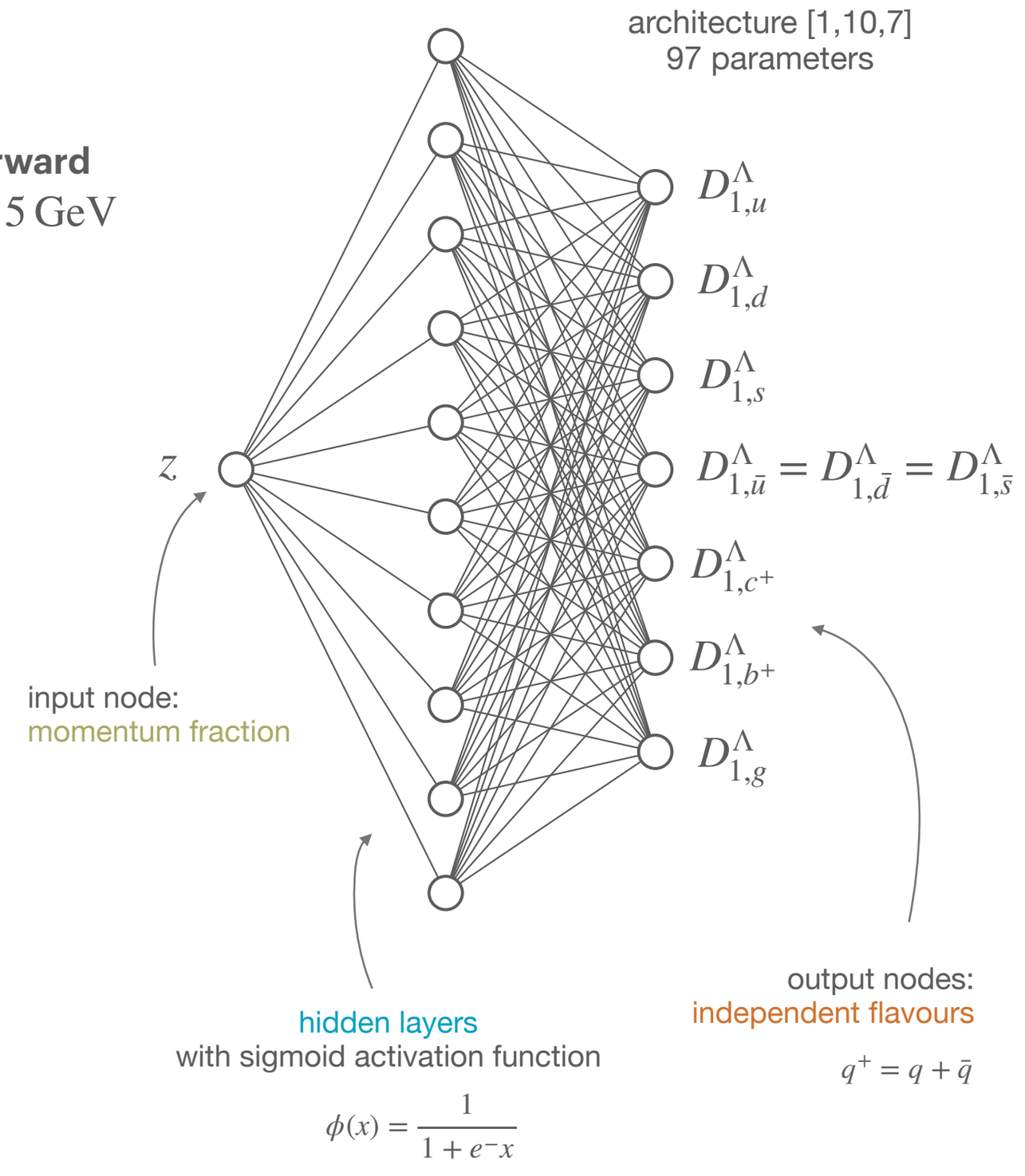

The MAPFF1.0 A fit

Fit quality

Experiment	$N_{\rm dat}$	$\chi^2/N_{\rm dat}$ NLO	$\chi^2/N_{\rm dat}$ NNLO
CHIO Λ	3	0.56	0.55
CHIO $\bar{\Lambda}$	4	1.11	1.03
EMC Λ	4	1.19	0.83
EMC $\bar{\Lambda}$	3	0.12	0.47
E665 Λ	3	0.50	0.48
E665 $\bar{\Lambda}$	3	1.00	1.27
H1 $\Lambda\bar{\Lambda}$	2	1.18	1.01
ZEUS $\Lambda\bar{\Lambda}$ 10-40	1	< 0.01	< 0.01
ZEUS $\Lambda\bar{\Lambda}$ 40-160	2	0.61	0.75
ZEUS $\Lambda\bar{\Lambda}$ 160-640	4	1.07	0.81
ZEUS $\Lambda\bar{\Lambda}$ 640-2560	3	0.46	0.37
ZEUS $\Lambda\bar{\Lambda}$ 2560-10240	1	0.03	0.03
WA59 Λ	6	0.34	0.33
NOMAD Λ	6	1.36	1.85
NOMAD $\bar{\Lambda}$	7	0.14	0.18
ABCMO Λ	4	4.05	3.05
ARGUS	16	1.49	1.55
Belle	15	1.13	1.26
TASSO 14	3	0.23	0.23
TASSO 22	4	0.48	0.49
TASSO 33	5	0.78	0.78
TASSO 34	7	0.57	0.56
TASSO 34.8	10	2.79	2.75
TASSO 42.1	4	1.13	1.12
HRS	12	0.82	0.82
MARK II	13	1.47	1.47
CELLO	7	0.52	0.51
ALEPH	25	0.48	0.44
DELPHI 91.2	10	2.62	2.58
OPAL	15	1.04	1.04
SLD	15	0.24	0.25
SLD UDS	8	2.30	2.02
SLD C	8	2.31	2.19
SLD B	8	0.50	0.80
Total	241	1.10	1.09

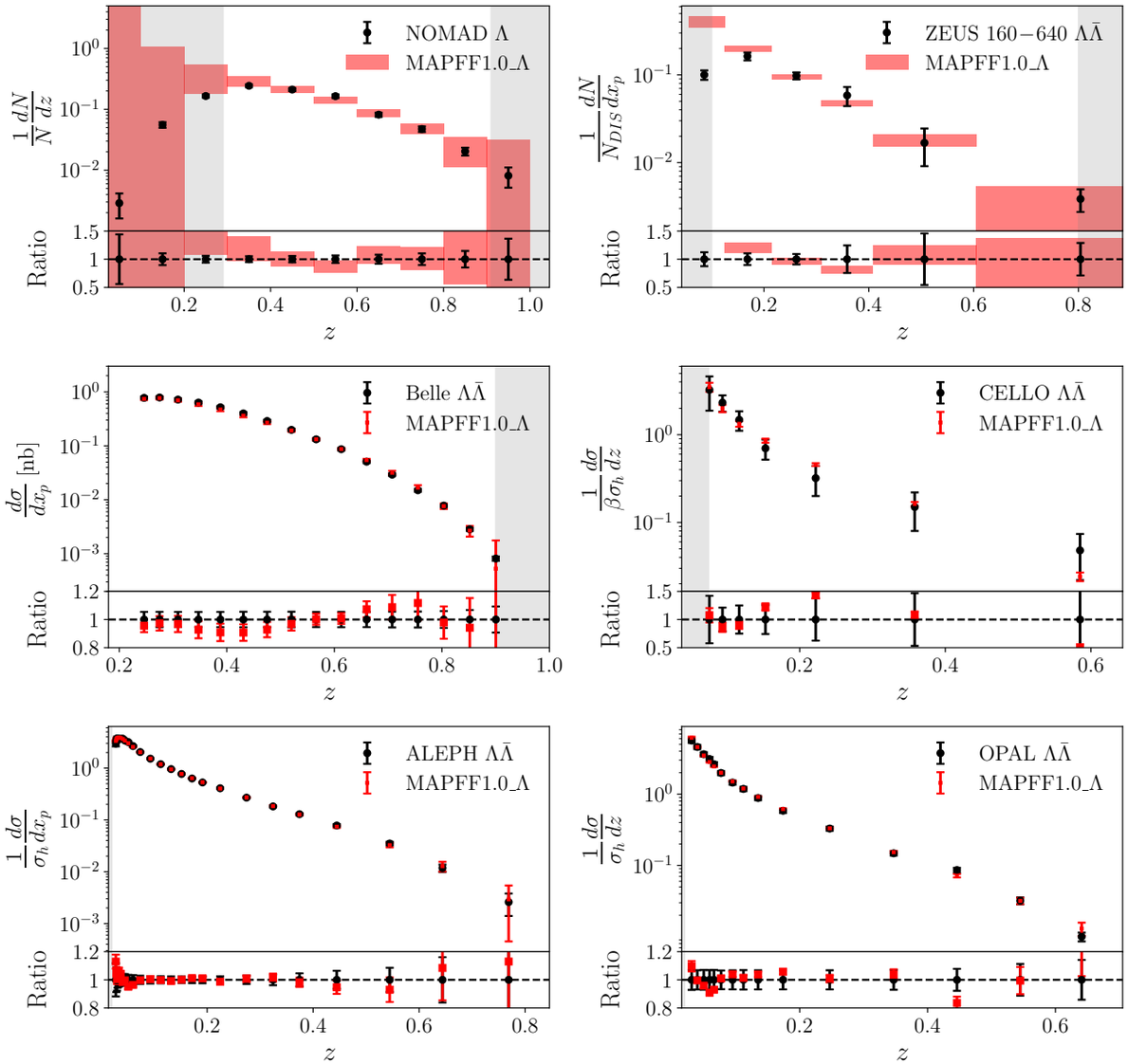

$\chi^2 = 1.10$ at NLO, $\chi^2 = 1.09$ at NNLO

Quality of the fit stable when going at NNLO
Slight improvement for the majority of the datasets

NLO vs NNLO

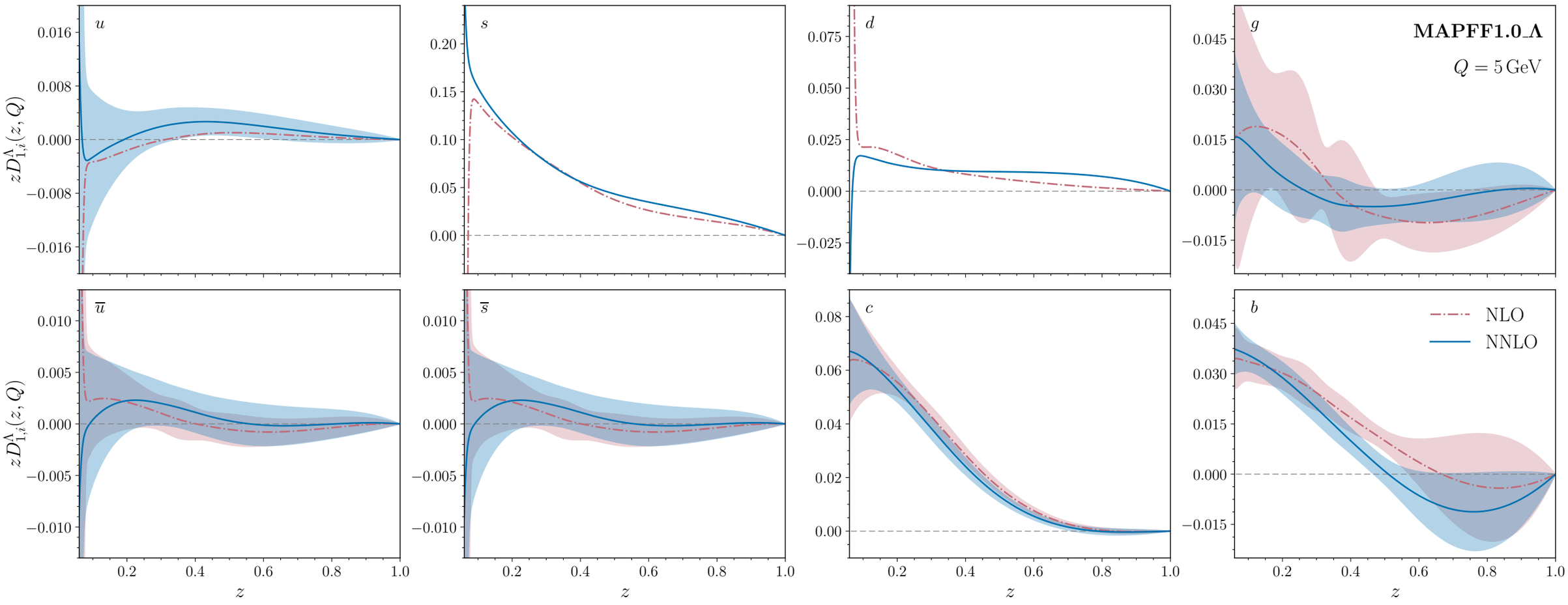
u
s
d
g
MAPFF1.0_Λ
$Q = 5\,\mathrm{GeV}$
$\overline{u}$
$\overline{s}$
c
b
NLO
NNLO
$zD^{\Lambda}_{1,i}(z,Q)$
z

NLO vs NNLO

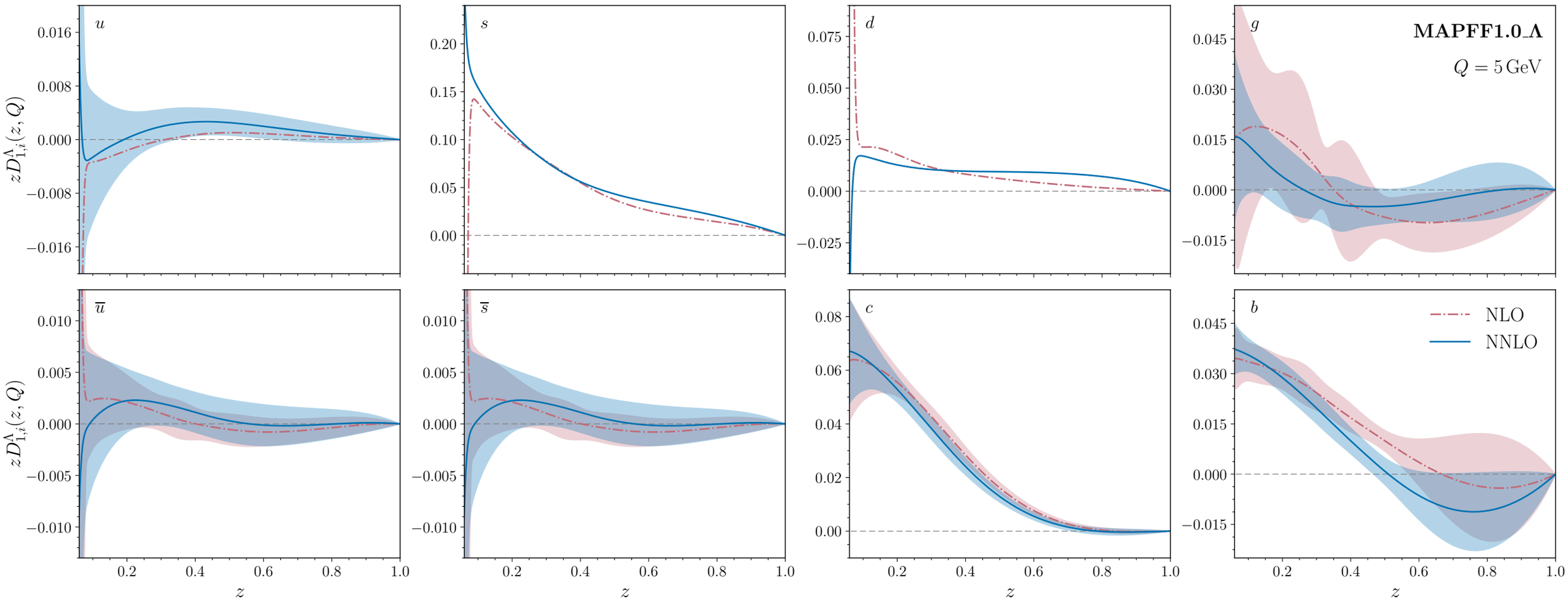

- **Light quarks** exhibit a slight positive shift going at NNLO

NLO vs NNLO

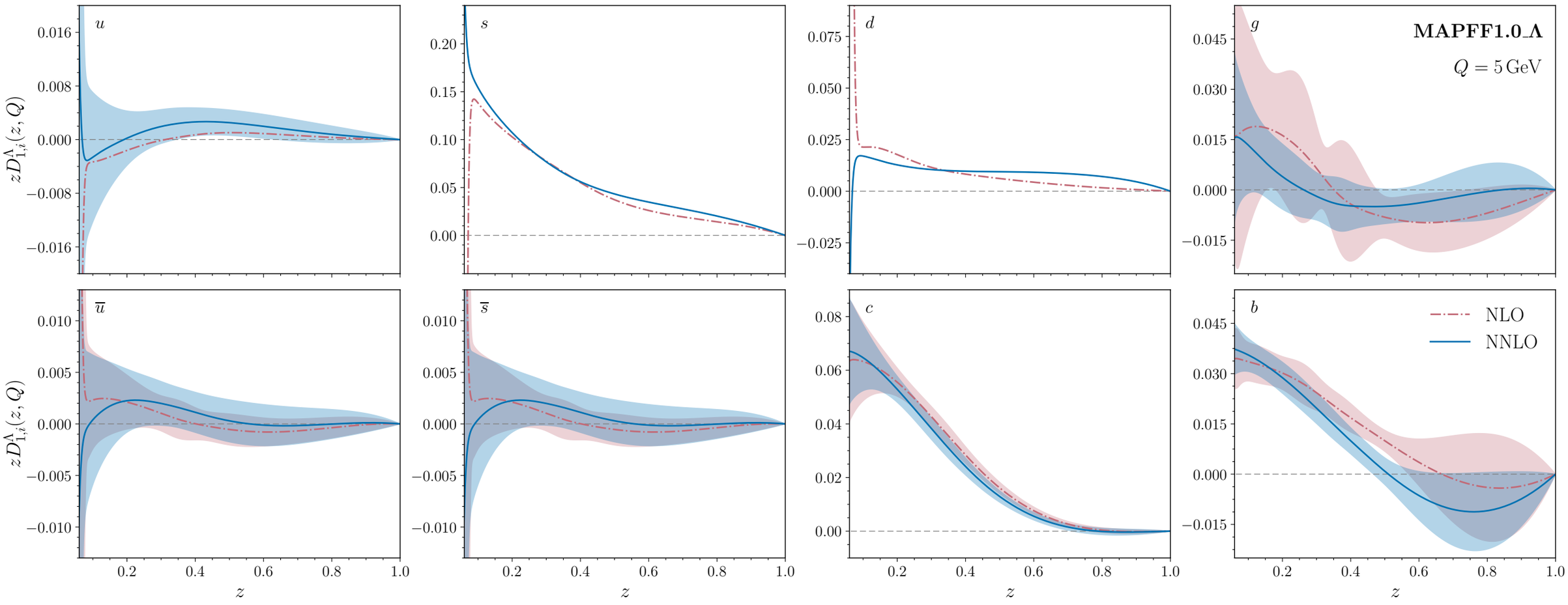

- **Light quarks** exhibit a slight positive shift going at NNLO
- The **gluon** is not well constrained, mostly compatible with zero

NLO vs NNLO

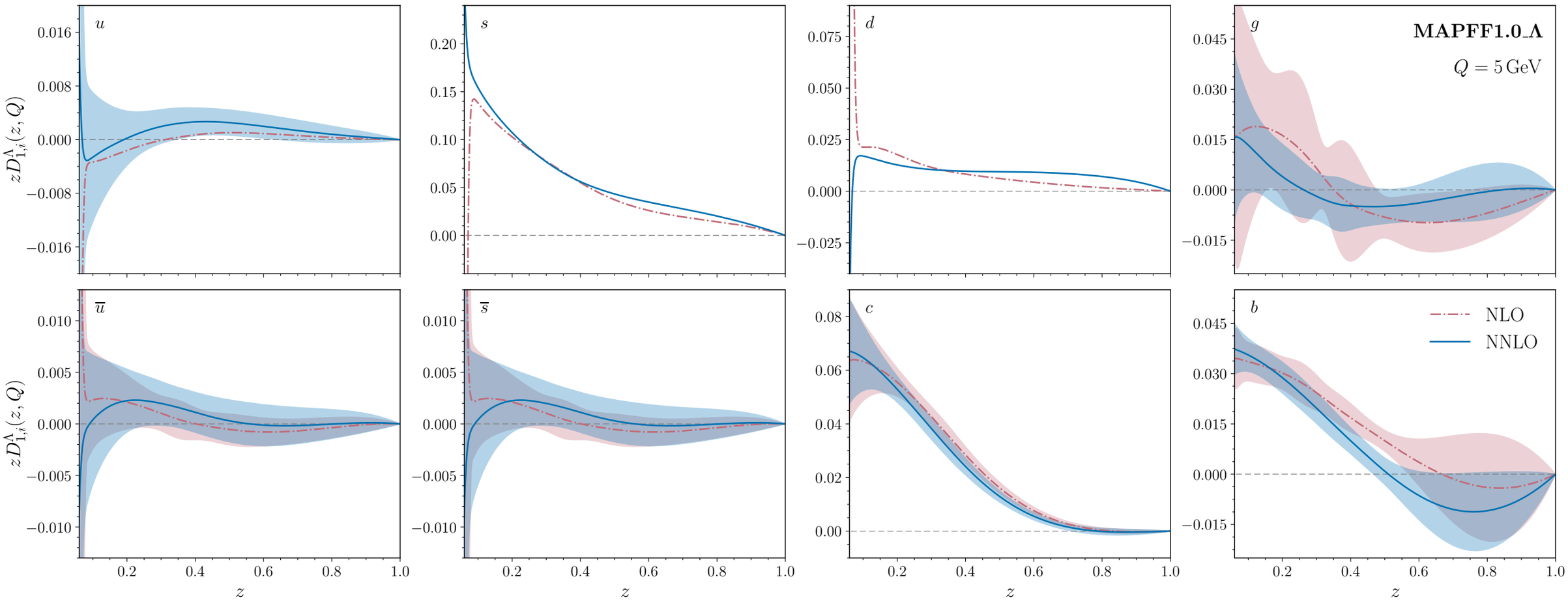

- **Light quarks** exhibit a slight positive shift going at NNLO
- The **gluon** is not well constrained, mostly compatible with zero
- **Charm** and **bottom** tend to shift downwards, bottom becomes negative at high z

NLO vs NNLO

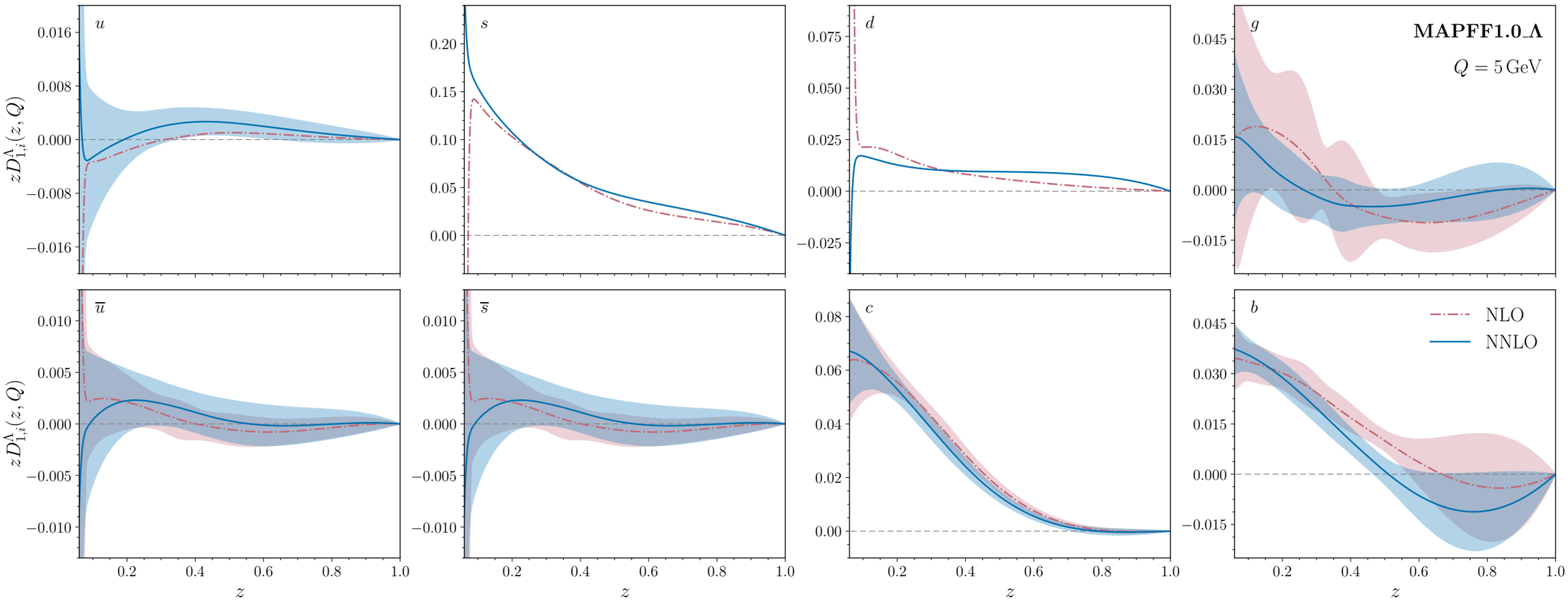

- **Light quarks** exhibit a slight positive shift going at NNLO
- The **gluon** is not well constrained, mostly compatible with zero
- **Charm** and **bottom** tend to shift downwards, bottom becomes negative at high z
- **Strange** quark uncertainty reduced when increasing perturbative accuracy

Valence quarks

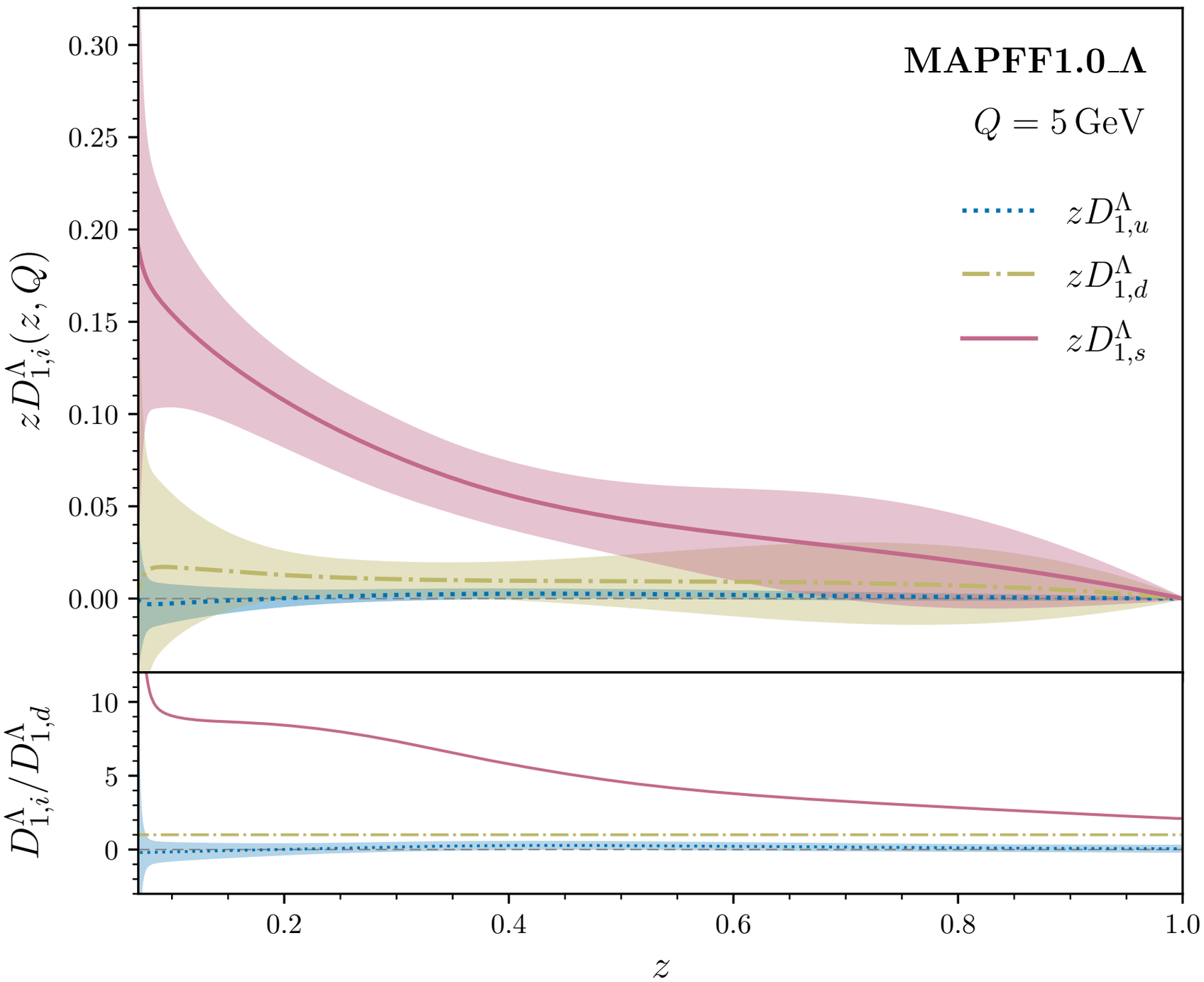

Valence quarks

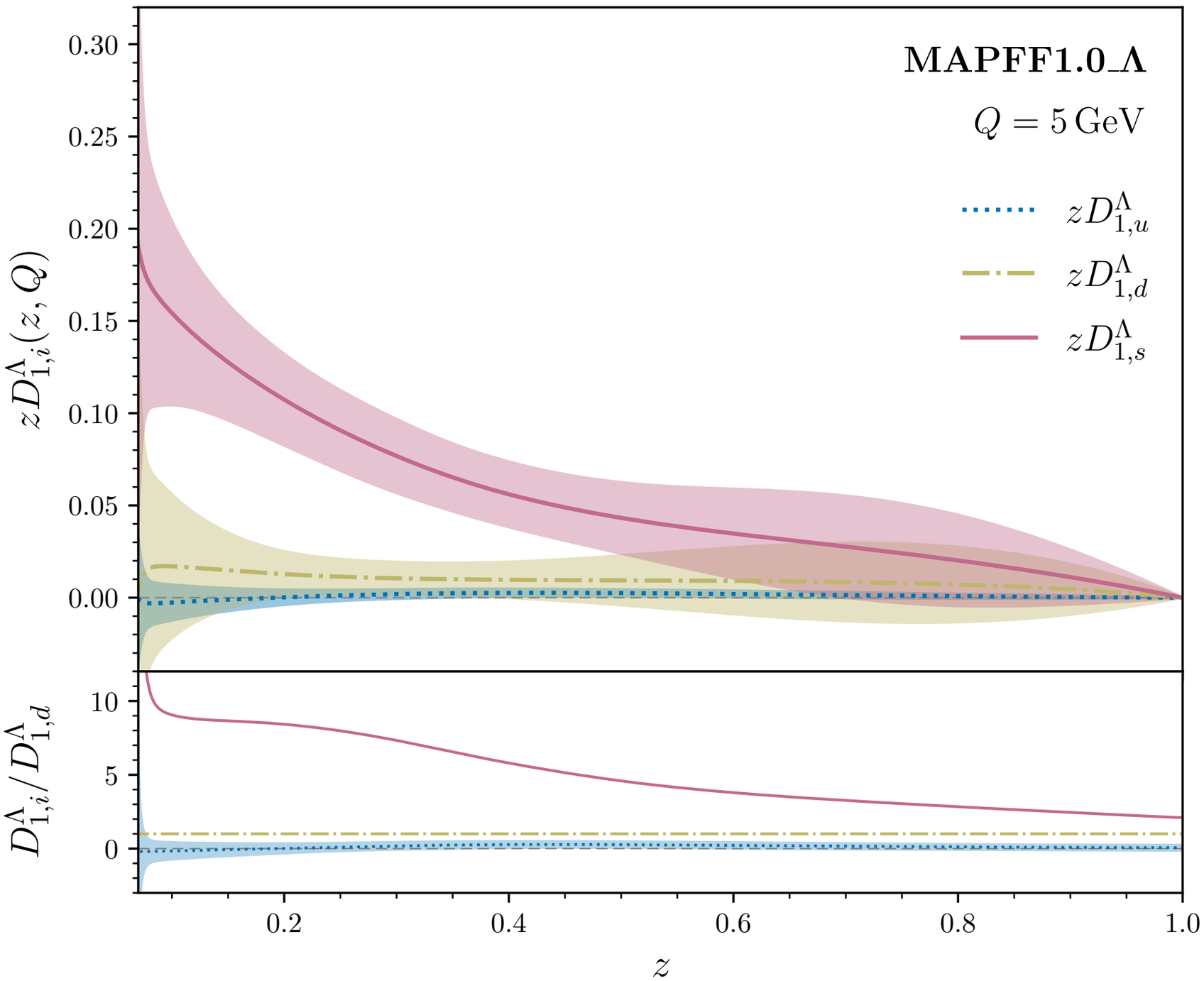

- **Dominance** of the strange quark over the entire z range: consistency with the quark composition of the Λ

Valence quarks

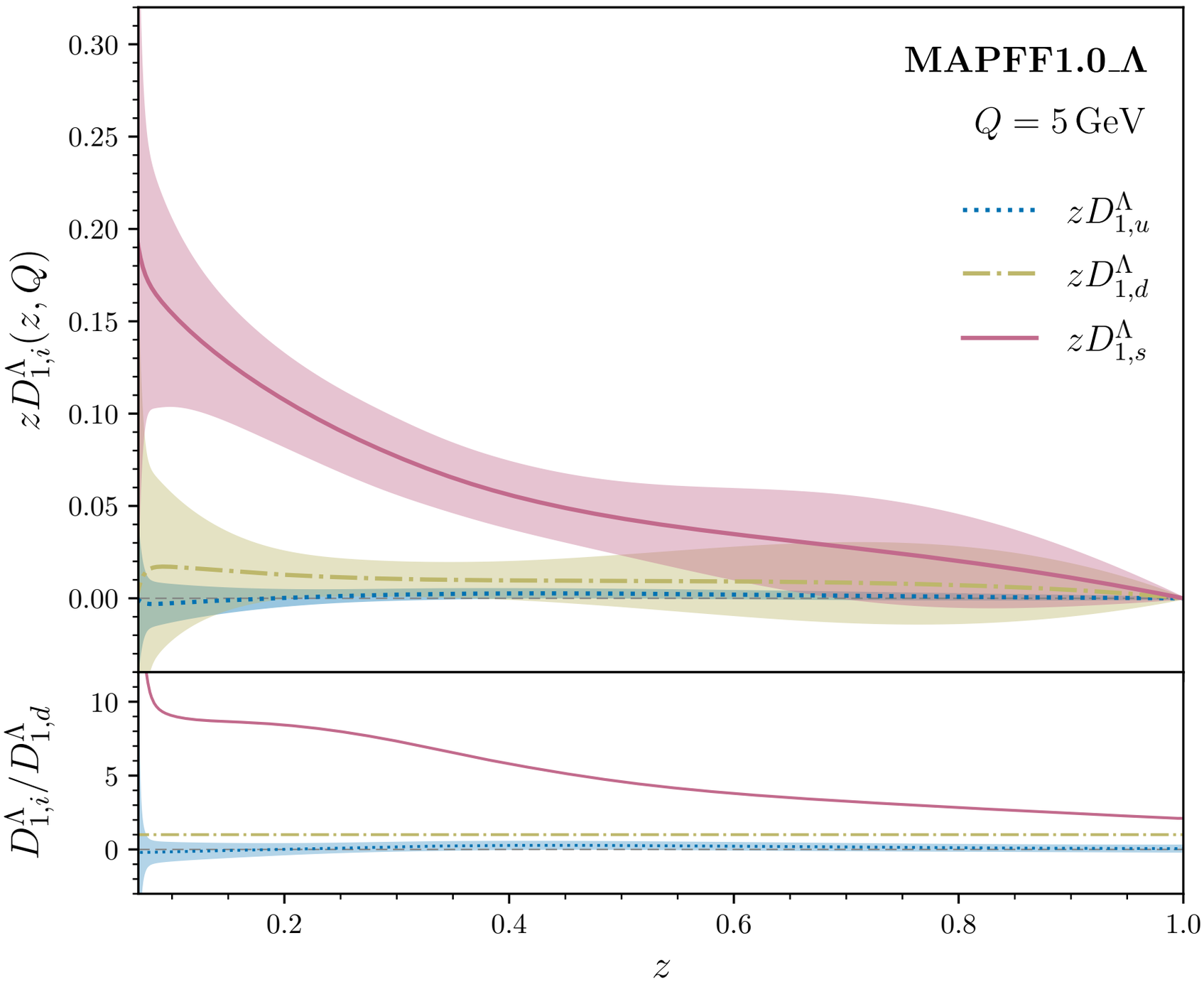

- **Dominance** of the strange quark over the entire z range: consistency with the quark composition of the Λ
- Fragmentation of u or d into Λ is less pronounced compared to s-quark fragmentation, the distributions show a similar shape

Positivity

Baseline: $z\, D^{\Lambda}_{1,i}(z,\mu_0) = \mathcal{N}_i(z,\theta) - \mathcal{N}_i(1,\theta)$ $\chi^2 = 1.09$

Positivity imposed: $z\, D^{\Lambda}_{1,i}(z,\mu_0) = (\mathcal{N}_i(z,\theta) - \mathcal{N}_i(1,\theta))^2$ $\chi^2 = 1.16$

Positivity

Baseline: $z\,D_{1,i}^{\Lambda}(z,\mu_0) = \mathcal{N}_i(z,\theta) - \mathcal{N}_i(1,\theta)$ $\quad \chi^2 = 1.09$

Positivity imposed: $z\,D_{1,i}^{\Lambda}(z,\mu_0) = (\mathcal{N}_i(z,\theta) - \mathcal{N}_i(1,\theta))^2$ $\quad \chi^2 = 1.16$

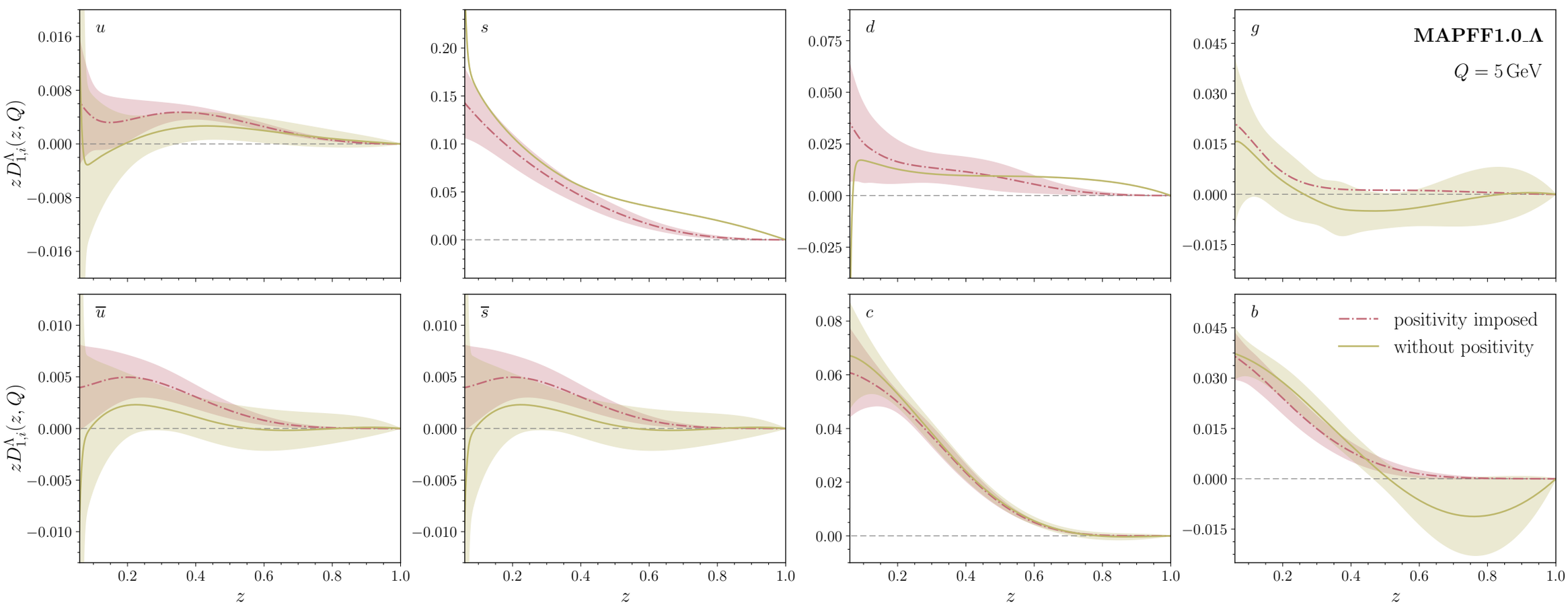

Positivity

Baseline: $z\,D_{1,i}^{\Lambda}(z,\mu_0) = \mathcal{N}_i(z,\theta) - \mathcal{N}_i(1,\theta) \qquad \chi^2 = 1.09$

Positivity imposed: $z\,D_{1,i}^{\Lambda}(z,\mu_0) = (\mathcal{N}_i(z,\theta) - \mathcal{N}_i(1,\theta))^2 \qquad \chi^2 = 1.16$

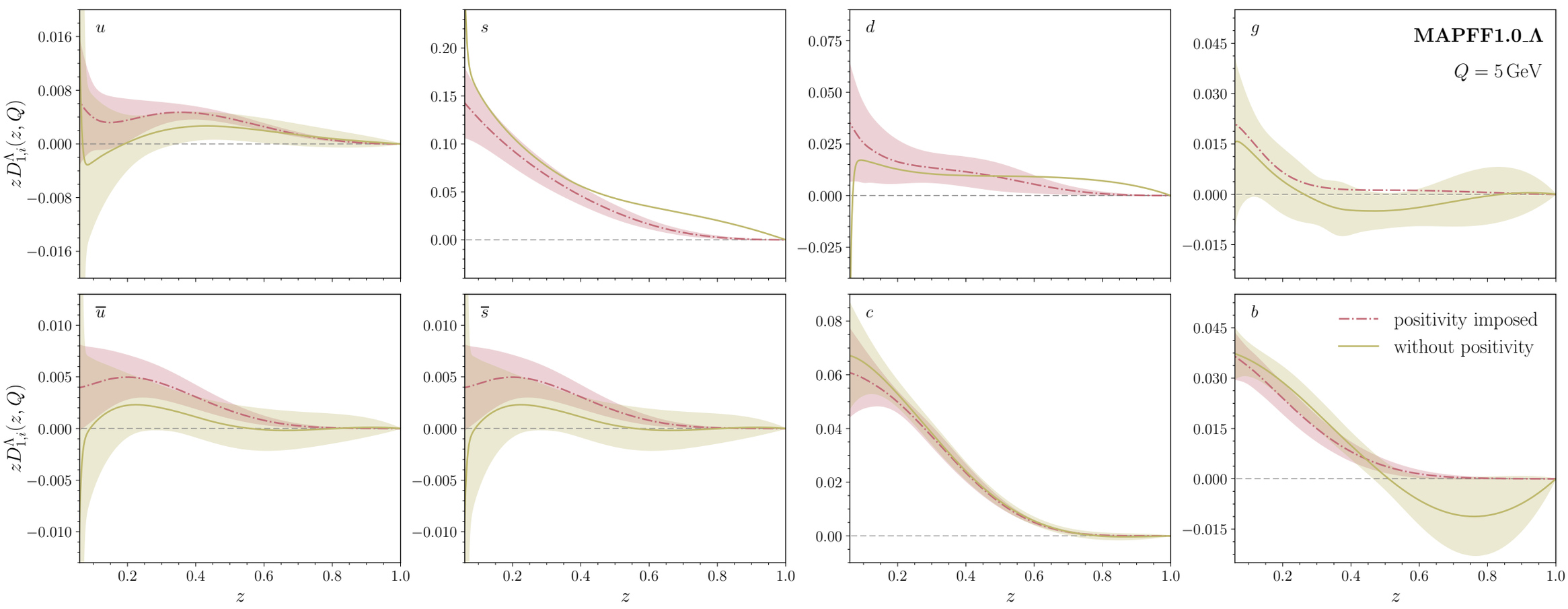

- Main effect of positivity requirement: **reduction of uncertainties' size** over the entire range in z

  More pronounced for large z and, for light quarks, also for $z < 0.1$, region constrained only from SIA

Positivity

Baseline: $z\,D_{1,i}^{\Lambda}(z,\mu_0) = \mathcal{N}_i(z,\theta) - \mathcal{N}_i(1,\theta) \qquad \chi^2 = 1.09$

Positivity imposed: $z\,D_{1,i}^{\Lambda}(z,\mu_0) = (\mathcal{N}_i(z,\theta) - \mathcal{N}_i(1,\theta))^2 \qquad \chi^2 = 1.16$

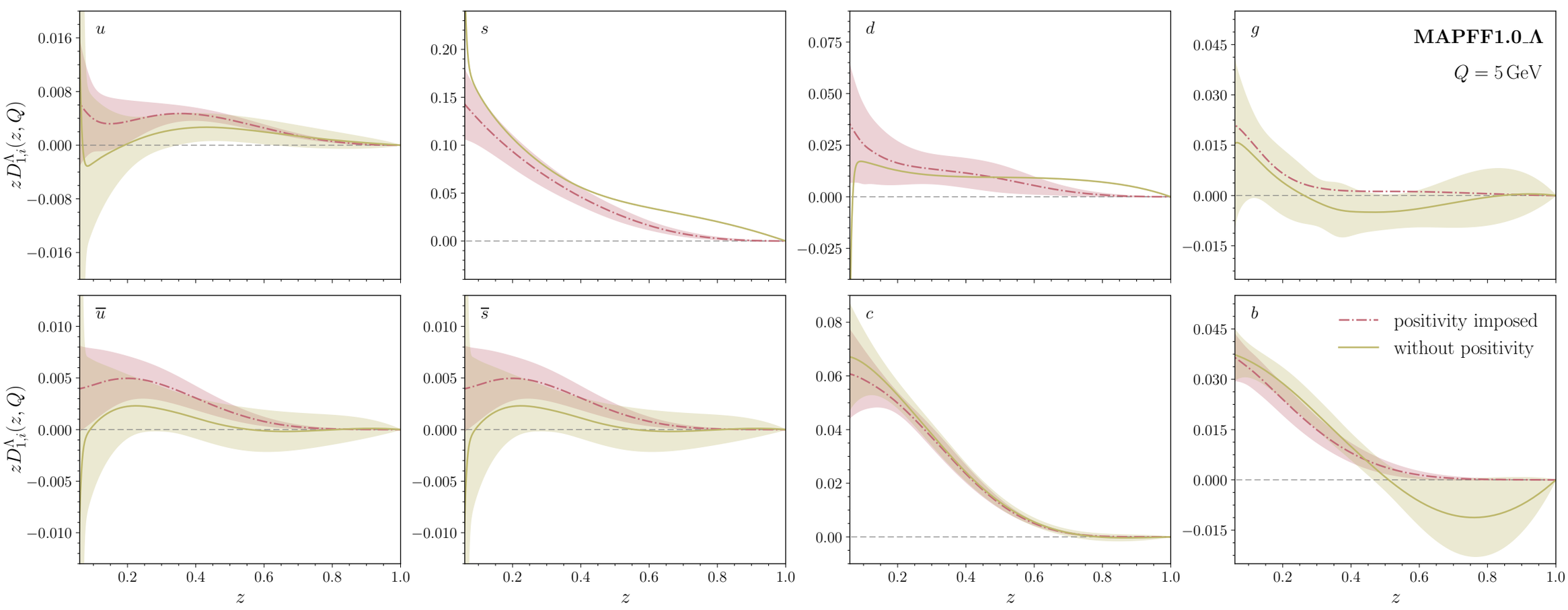

- Main effect of positivity requirement: **reduction of uncertainties' size** over the entire range in z

  More pronounced for large z and, for light quarks, also for $z < 0.1$, region constrained only from SIA

- **Shape** overall **preserved** by the positivity requirement

Positivity: replicas

Study of positivity effect for the single replicas

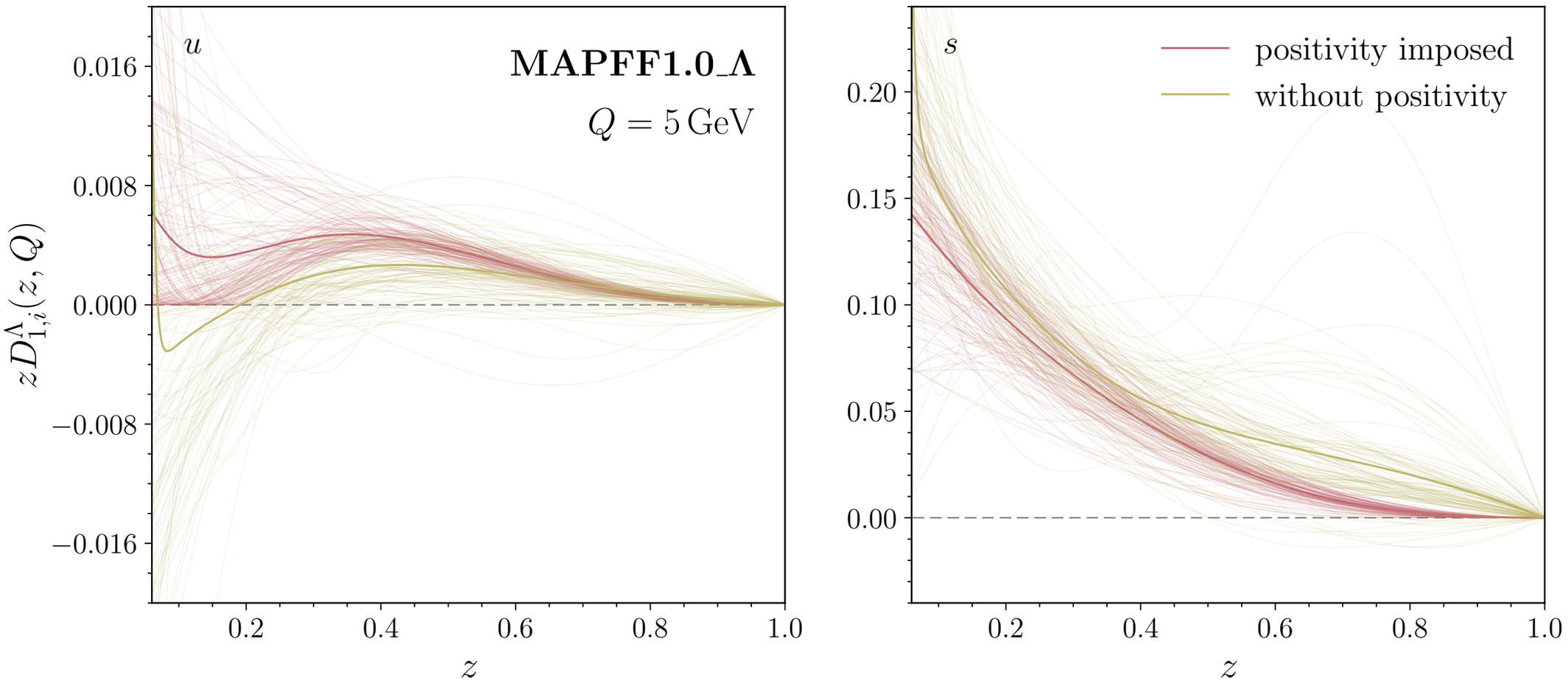

Positivity: replicas

Study of positivity effect for the single replicas

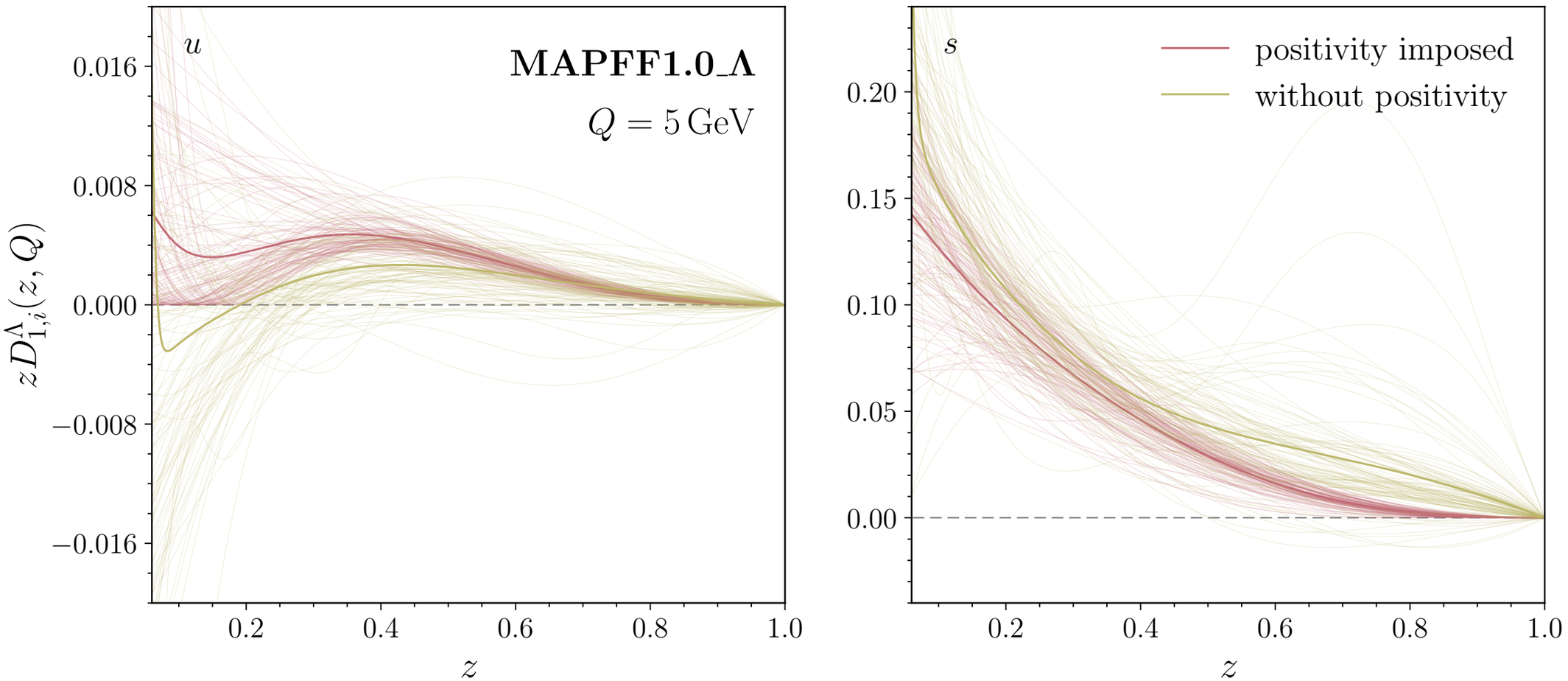

- Tendency of up quark replicas at low z to become negative for the baseline fit

Positivity: replicas

Study of positivity effect for the single replicas

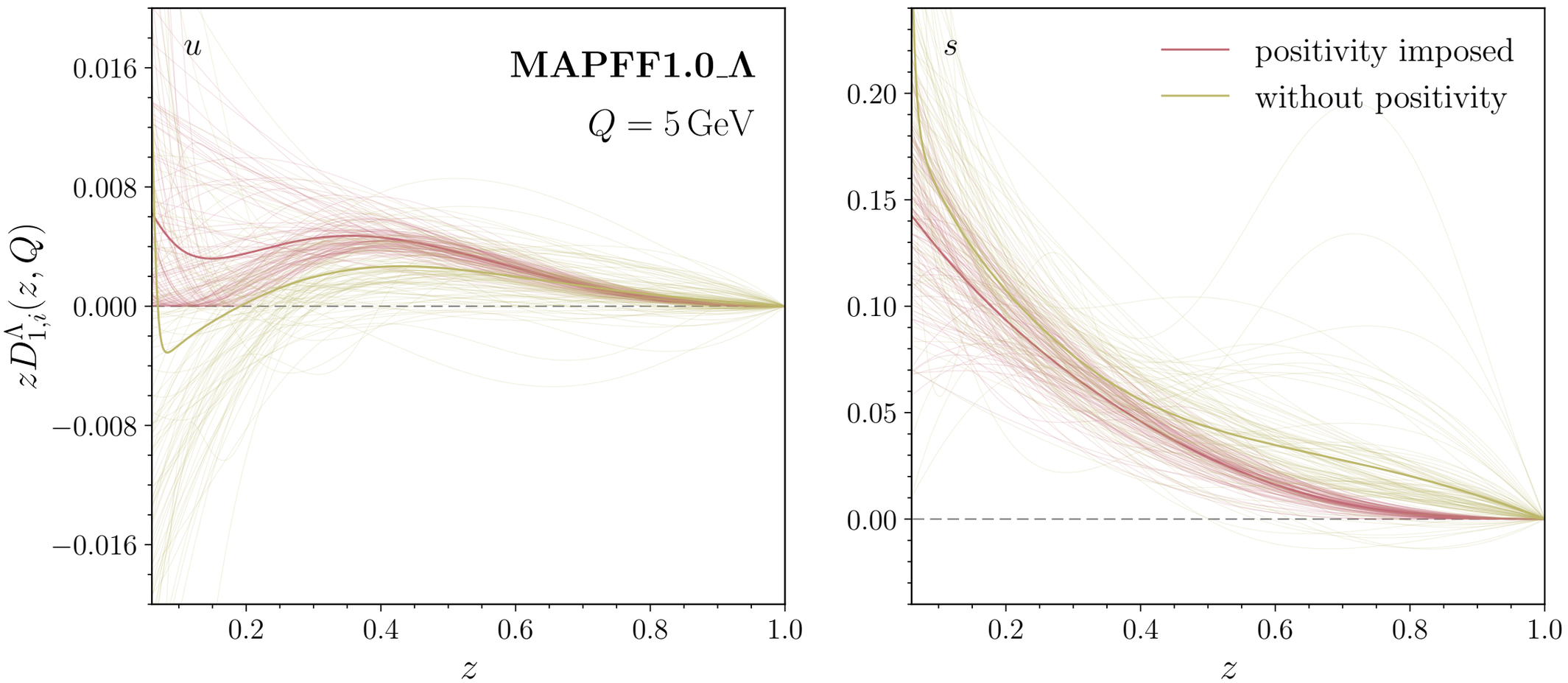

- Tendency of up quark replicas at low z to become negative for the baseline fit
- Wider spread for strange quark replicas for the baseline fit, compatible distributions overall

Comparison at NLO with other FFs

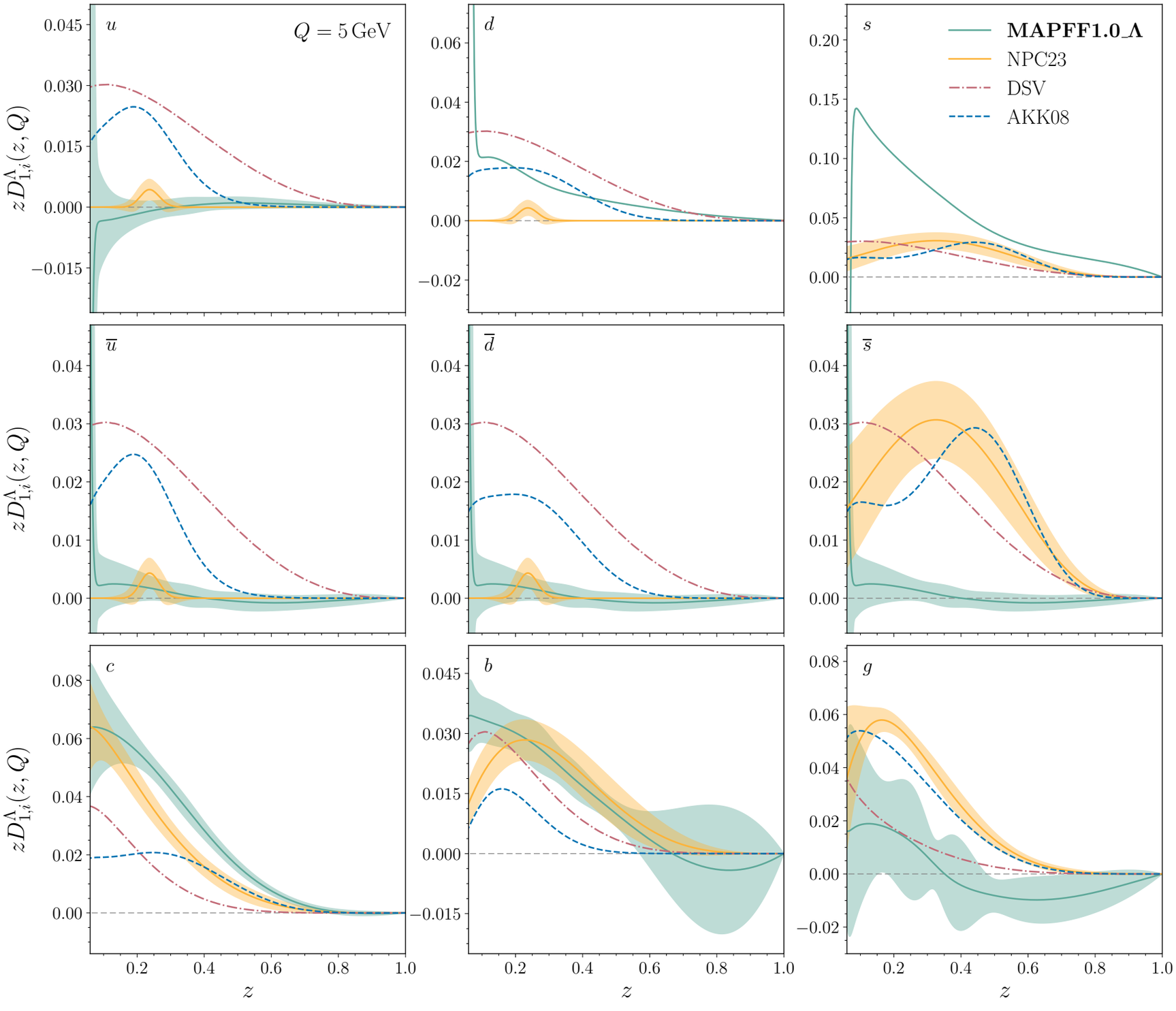

Comparison at NLO with other FFs

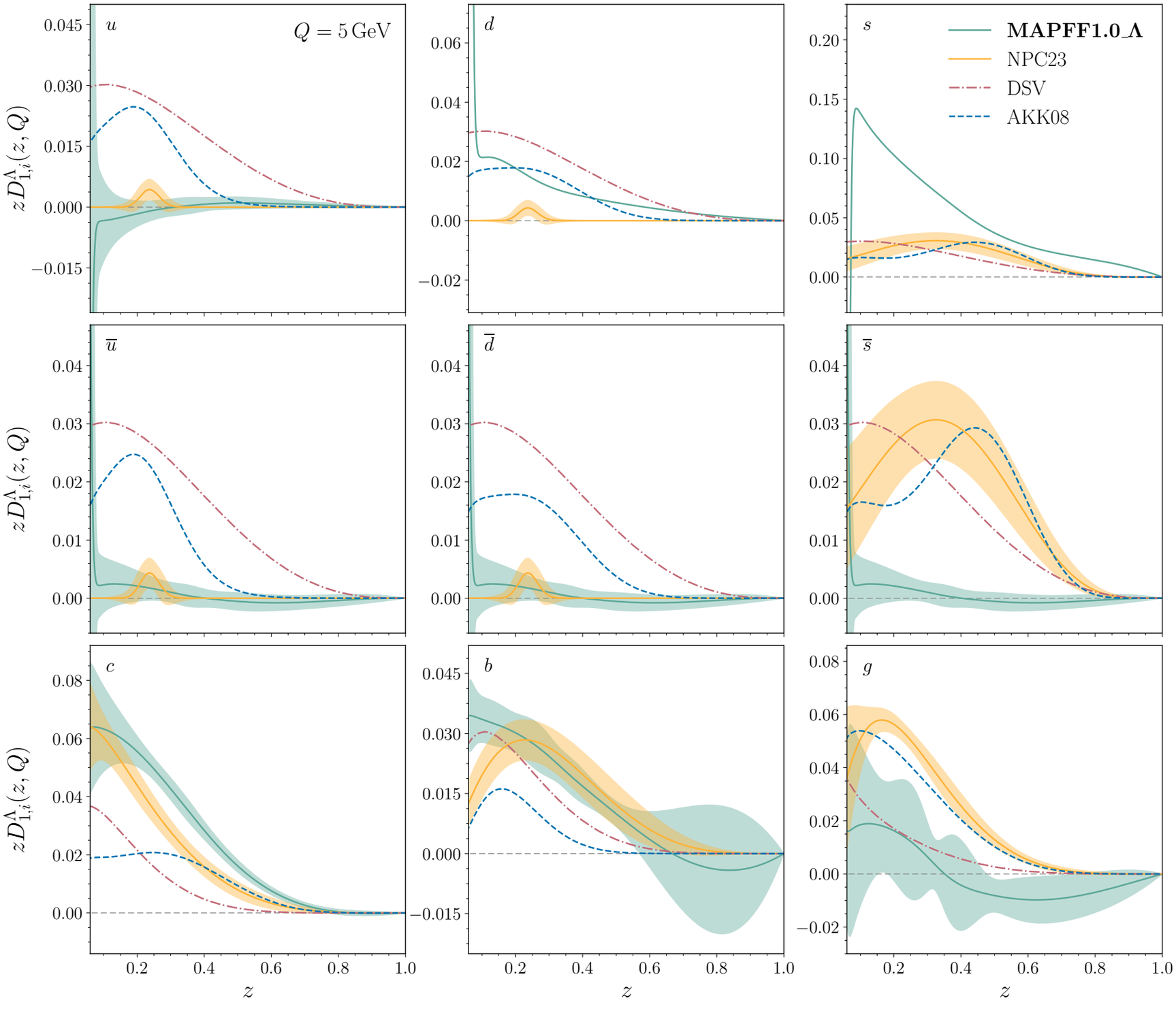

Good overall **agreement** for $D^{\Lambda}_{1,d}$

Comparison at NLO with other FFs

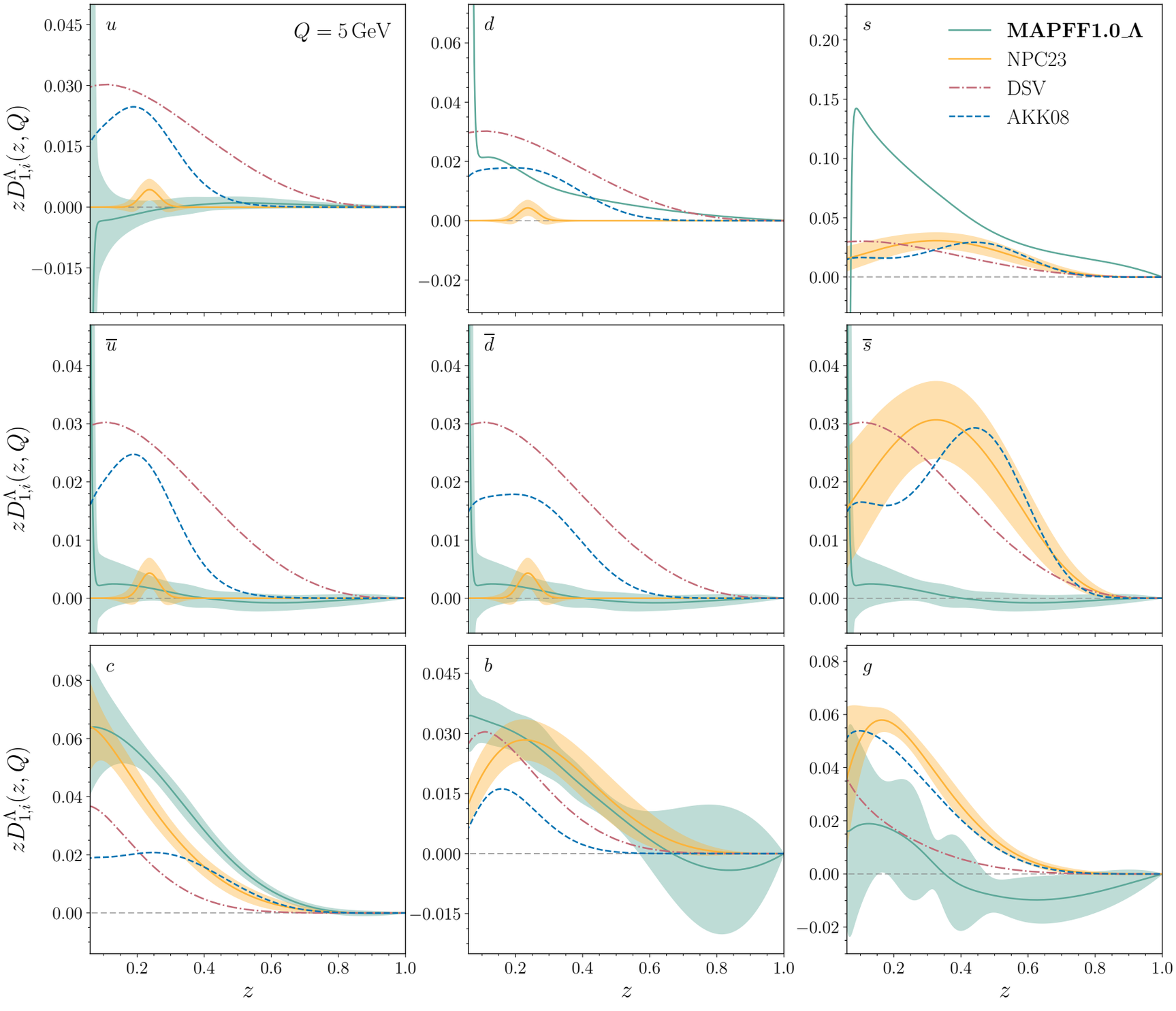

Good overall **agreement** for $D^{\Lambda}_{1,d}$

Suppression of the $D^{\Lambda}_{1,u}$ w.r.t. the other extractions

Comparison at NLO with other FFs

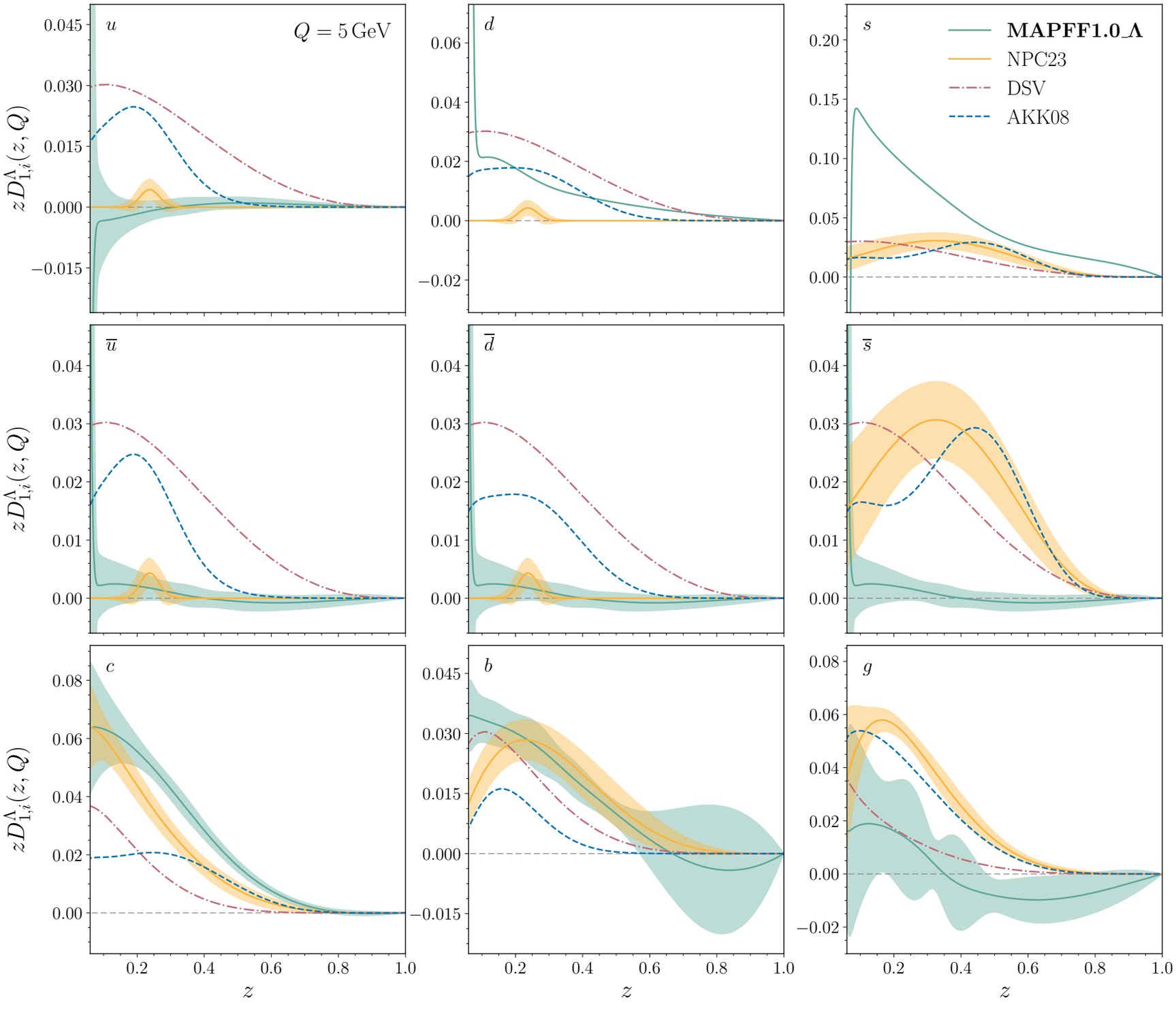

Good overall **agreement** for $D^{\Lambda}_{1,d}$

Suppression of the $D^{\Lambda}_{1,u}$ w.r.t. the other extractions

Choice of independent parameterisation for $D^{\Lambda}_{1,s}$ reflects in the **dominance** over the other two valence quarks

Comparison at NLO with other FFs

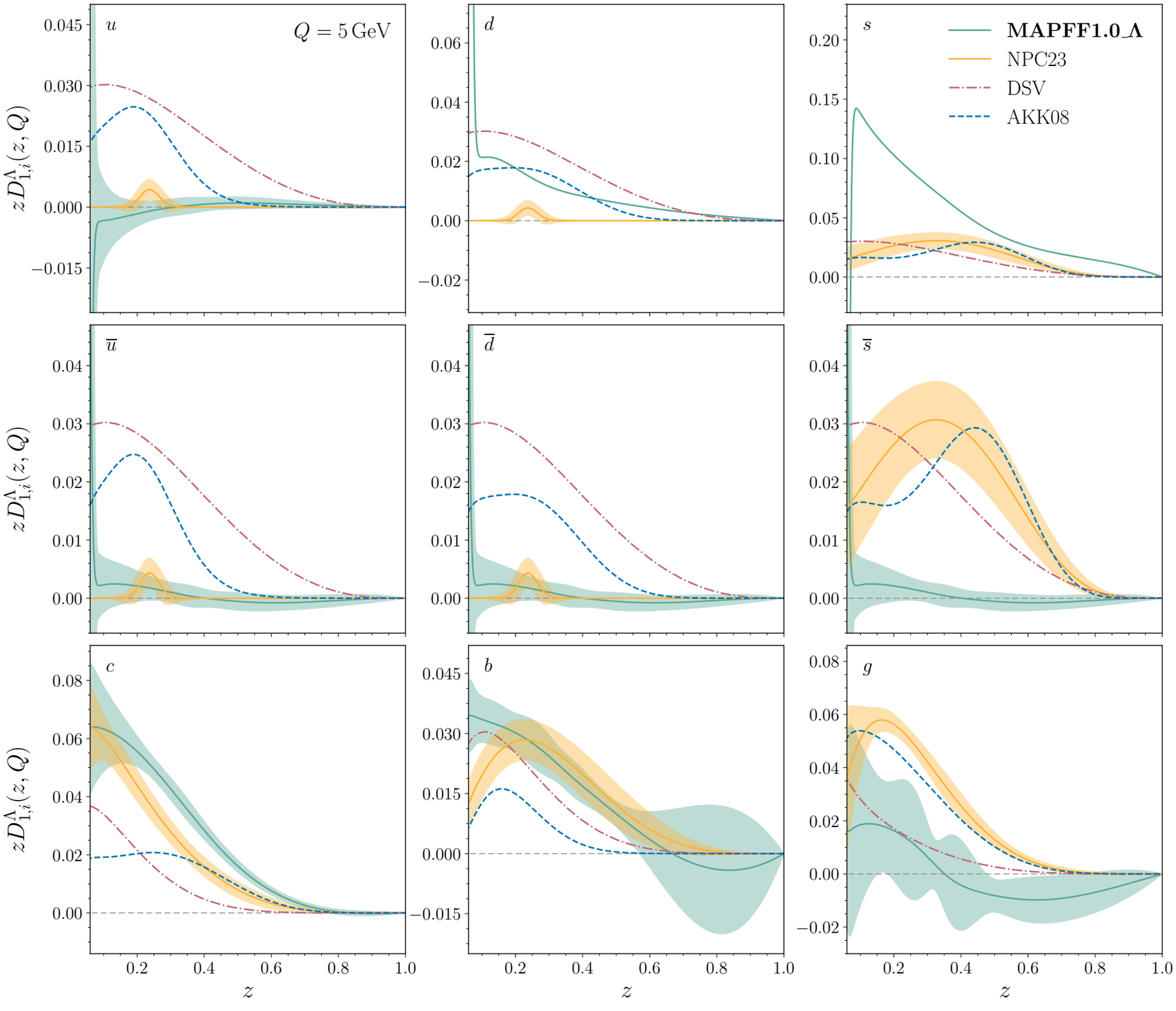

Good overall **agreement** for $D^{\Lambda}_{1,d}$

Suppression of the $D^{\Lambda}_{1,u}$ w.r.t. the other extractions

Choice of independent parameterisation for $D^{\Lambda}_{1,s}$ reflects in the **dominance** over the other two valence quarks

Marked **discrepancy** for the sea quarks for different parameterisation choice

Comparison at NLO with other FFs

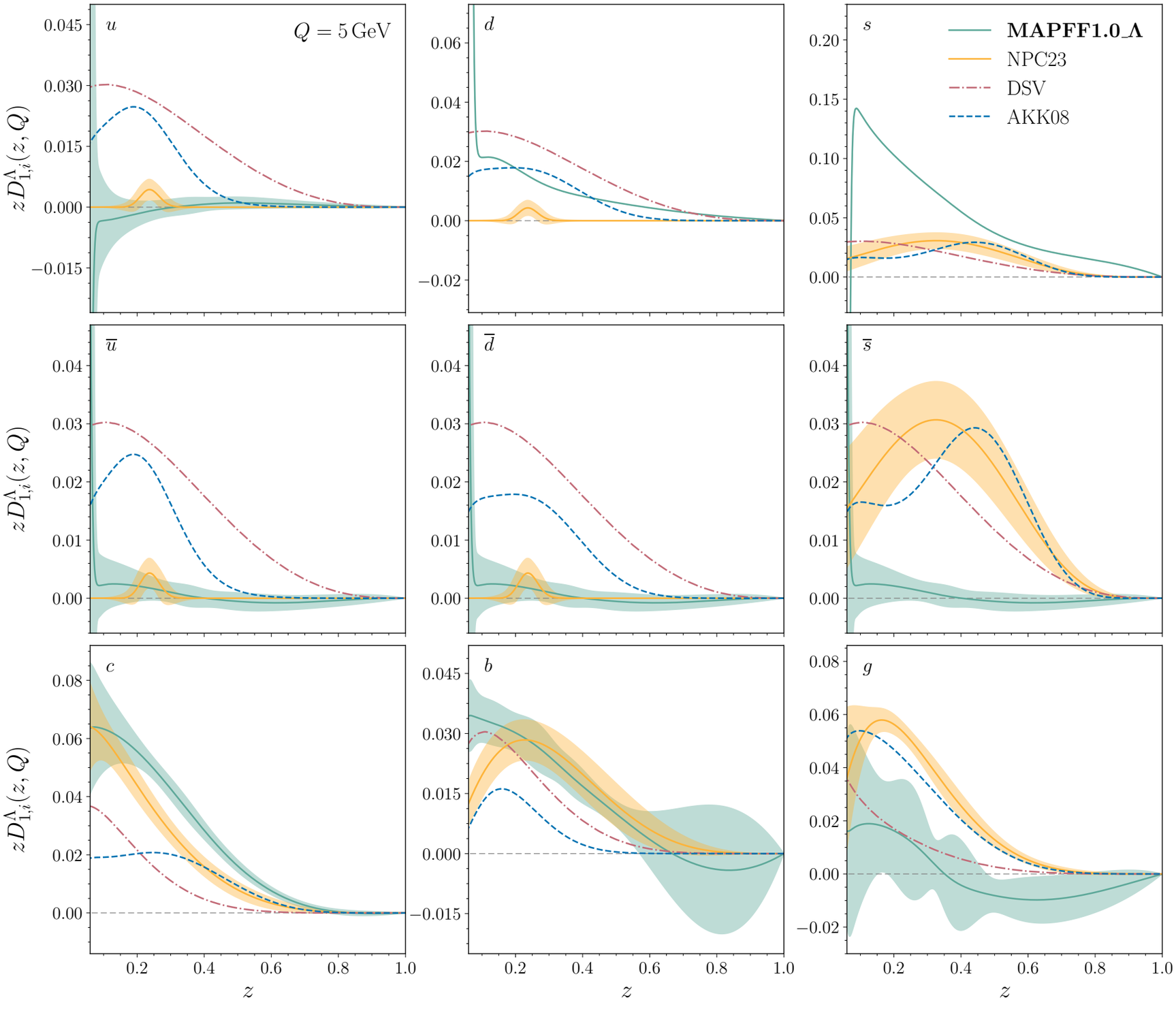

Good overall **agreement** for $D^{\Lambda}_{1,d}$

Suppression of the $D^{\Lambda}_{1,u}$ w.r.t. the other extractions

Choice of independent parameterisation for $D^{\Lambda}_{1,s}$ reflects in the **dominance** over the other two valence quarks

Marked **discrepancy** for the sea quarks for different parameterisation choice

Good **agreement** for c and b

Comparison at NLO with other FFs

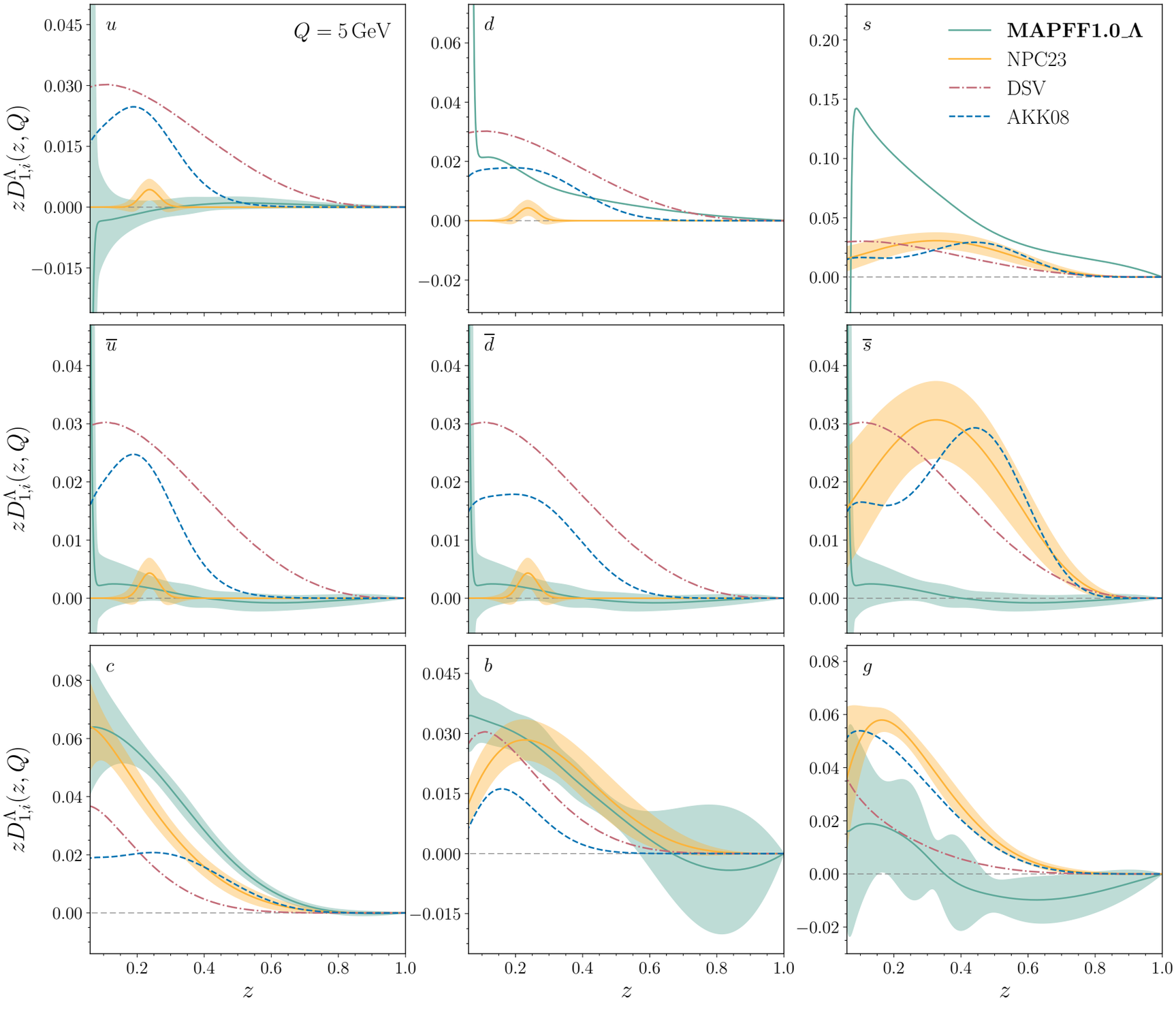

Good overall **agreement** for $D^{\Lambda}_{1,d}$

Suppression of the $D^{\Lambda}_{1,u}$ w.r.t. the other extractions

Choice of independent parameterisation for $D^{\Lambda}_{1,s}$ reflects in the **dominance** over the other two valence quarks

Marked **discrepancy** for the sea quarks for different parameterisation choice

Good **agreement** for c and b

Gluon poorly constrained

Summary

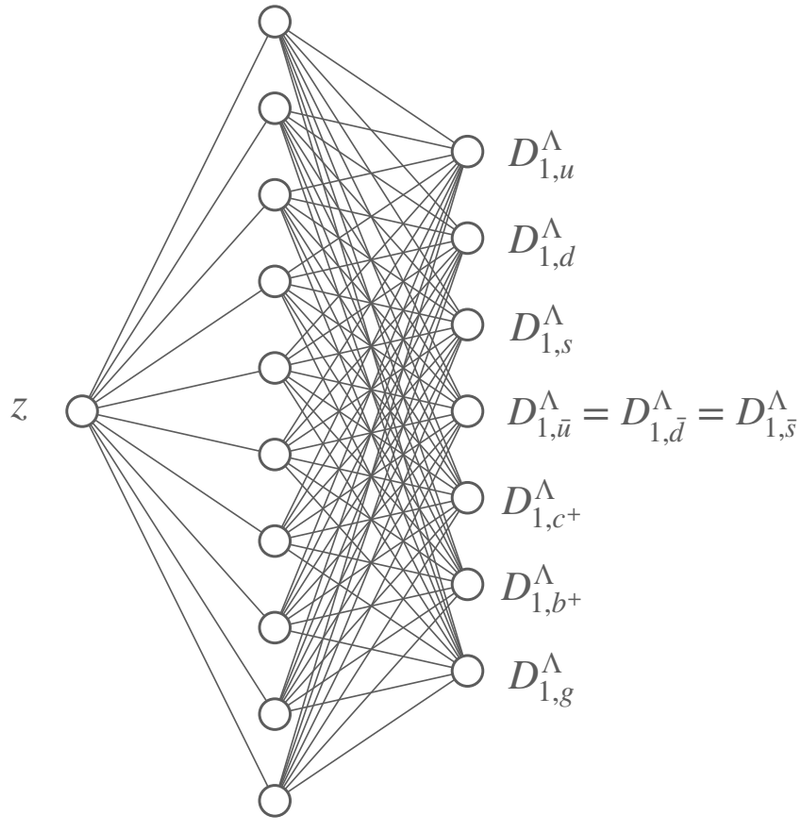
z
$D^{\Lambda}_{1,u}$
$D^{\Lambda}_{1,d}$
$D^{\Lambda}_{1,s}$
$D^{\Lambda}_{1,\bar{u}} = D^{\Lambda}_{1,\bar{d}} = D^{\Lambda}_{1,\bar{s}}$
D^{Λ}_{1,c^+}
D^{Λ}_{1,b^+}
$D^{\Lambda}_{1,g}$

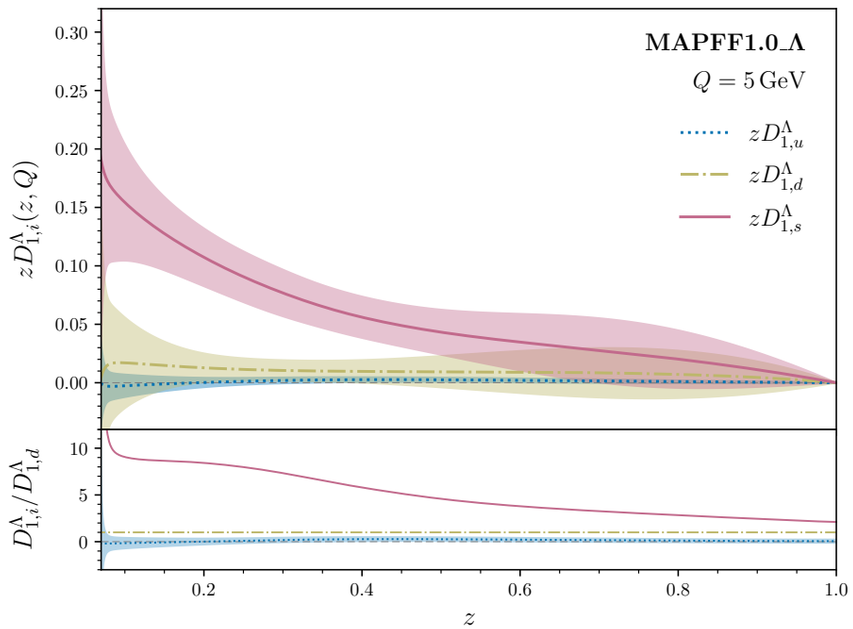
MAPFF1.0_Λ
$Q = 5\,\mathrm{GeV}$
$zD^{\Lambda}_{1,u}$
$zD^{\Lambda}_{1,d}$
$zD^{\Lambda}_{1,s}$
$zD^{\Lambda}_{1,i}(z,Q)$
$D^{\Lambda}_{1,i}/D^{\Lambda}_{1,d}$
z

Summary

- Global analysis at next-to-next-to-leading order of perturbative accuracy of the **collinear unpolarised FFs for Λ hyperons**

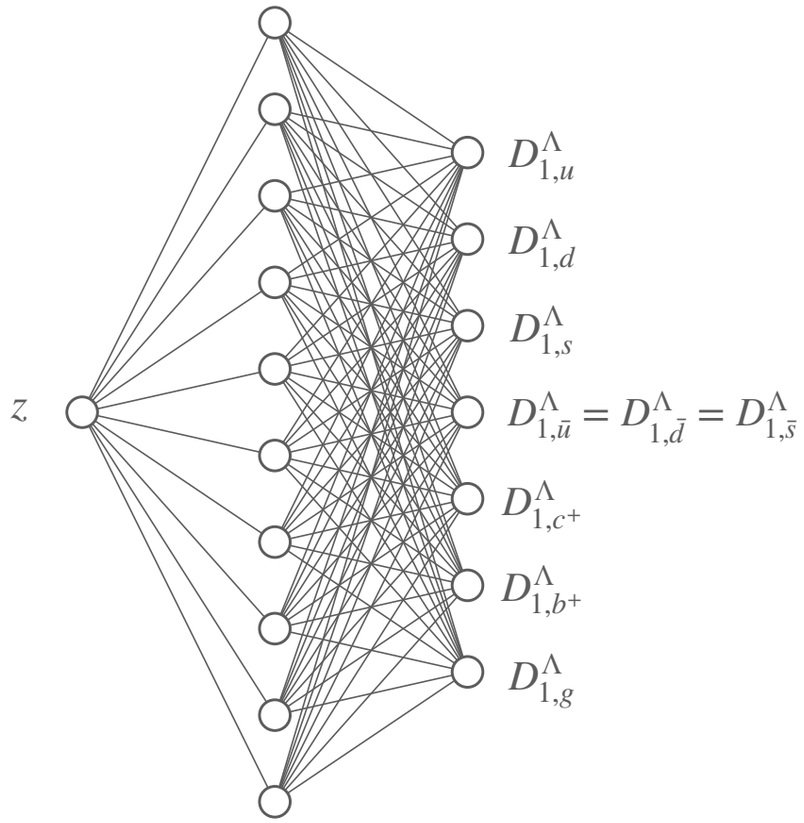

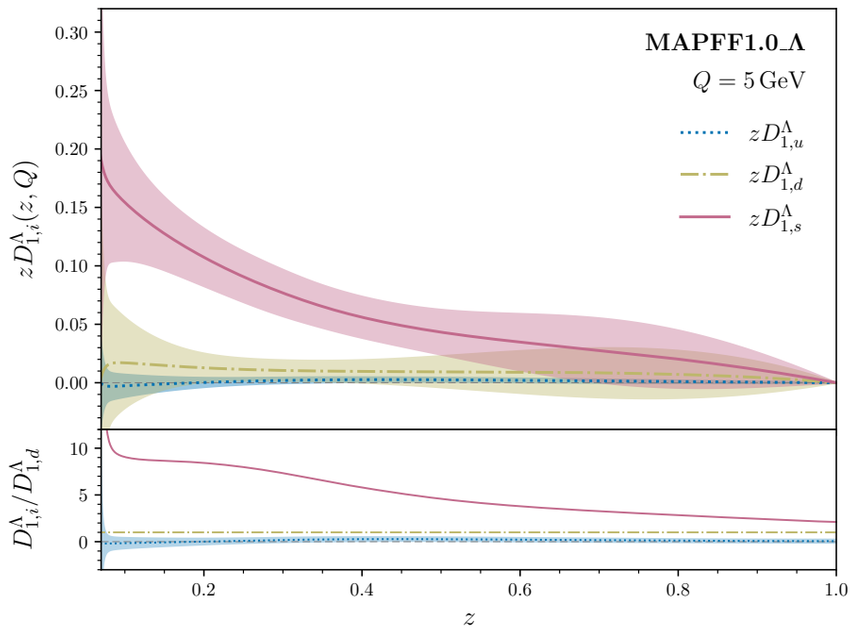

Summary

- Global analysis at next-to-next-to-leading order of perturbative accuracy of the **collinear unpolarised FFs for Λ hyperons**
- The fit is based on experimental data from SIA and both neutral-current and — for the first time — **charged-current SIDIS**.

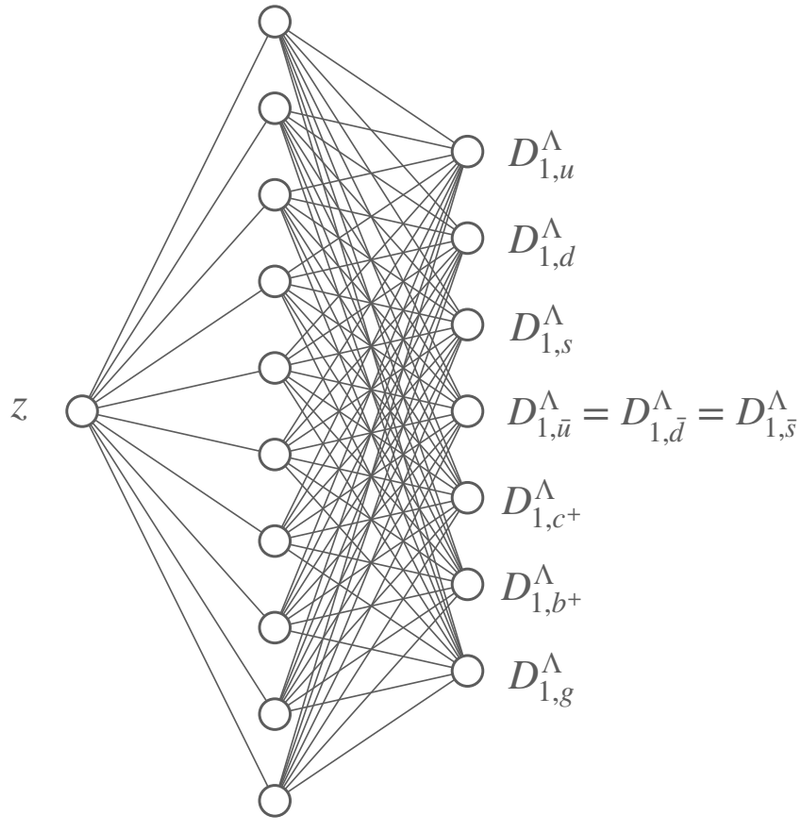

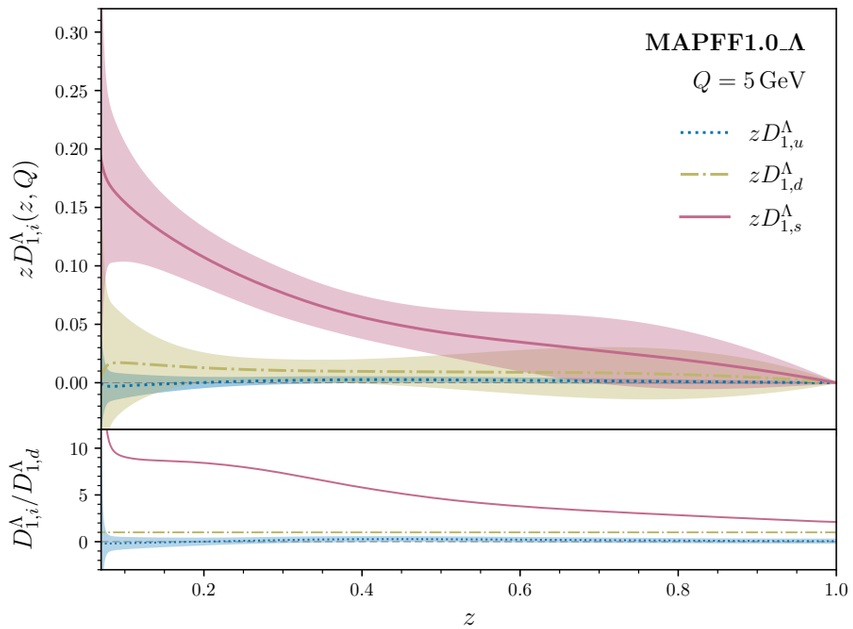

Summary

- Global analysis at next-to-next-to-leading order of perturbative accuracy of the **collinear unpolarised FFs for Λ hyperons**
- The fit is based on experimental data from SIA and both neutral-current and — for the first time — **charged-current SIDIS**.
- Statistical framework based on the Monte Carlo sampling method and FFs parameterisation in terms of a **neural network** that comprises a total of seven independent flavours.

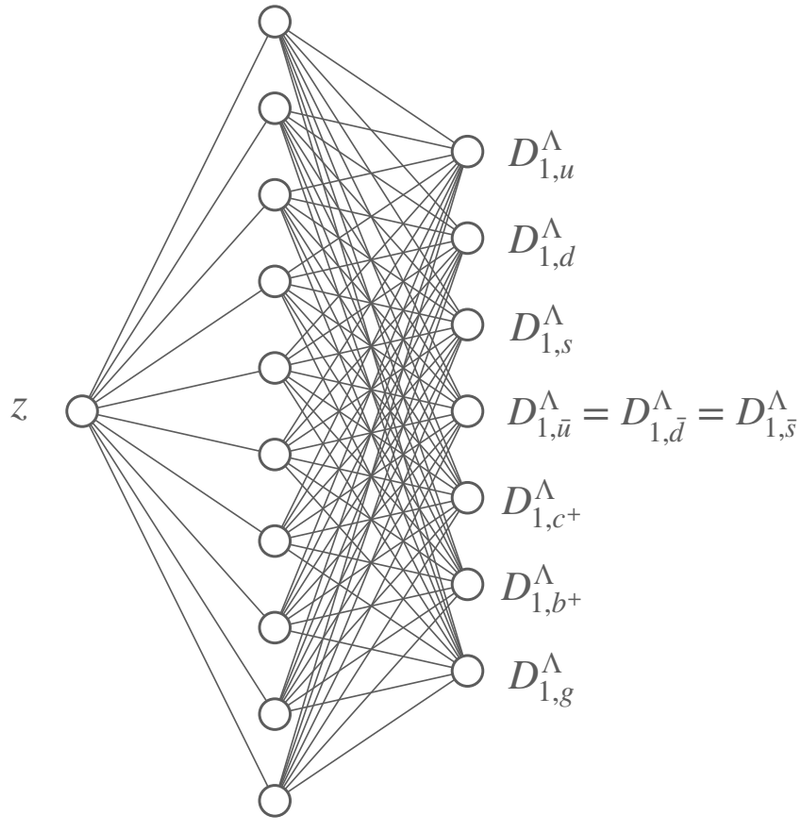

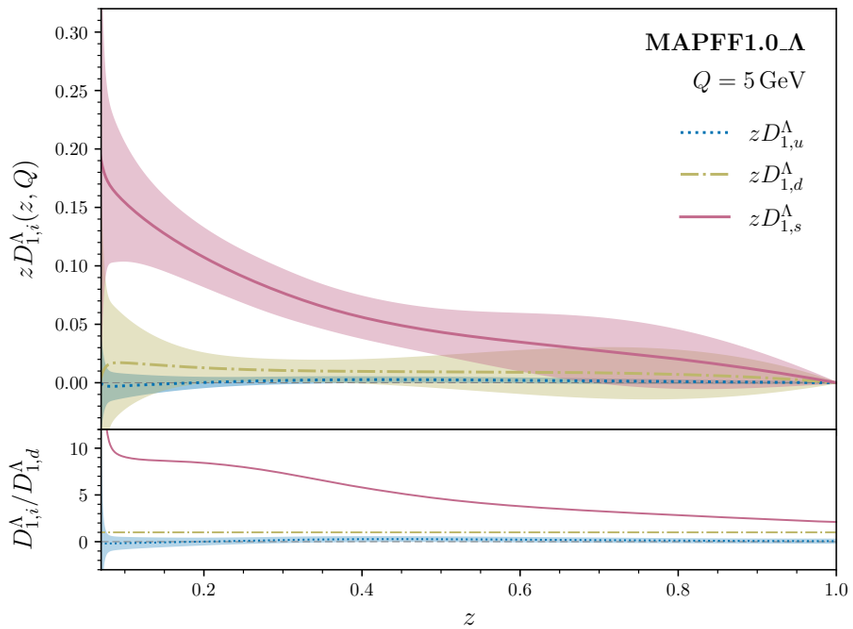

Summary

- Global analysis at next-to-next-to-leading order of perturbative accuracy of the **collinear unpolarised FFs for Λ hyperons**

- The fit is based on experimental data from SIA and both neutral-current and — for the first time — **charged-current SIDIS**.

- Statistical framework based on the Monte Carlo sampling method and FFs parameterisation in terms of a **neural network** that comprises a total of seven independent flavours.

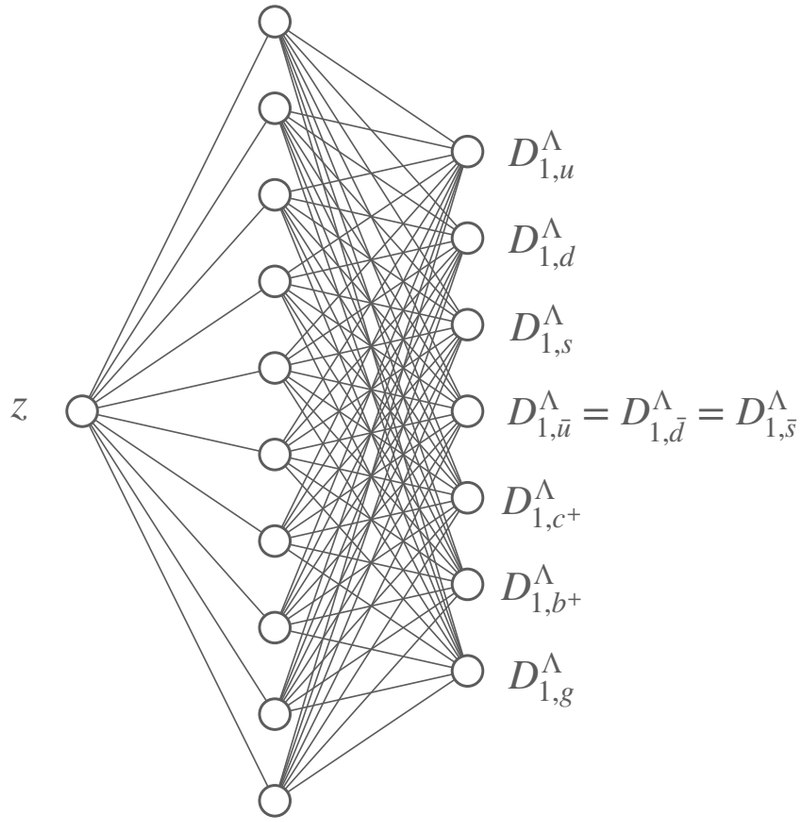

- First determination for the Λ and $\bar{\Lambda}$ **separately**, offering new insights into the hadronisation mechanism of strange baryons and establishing a baseline for future phenomenological investigations.

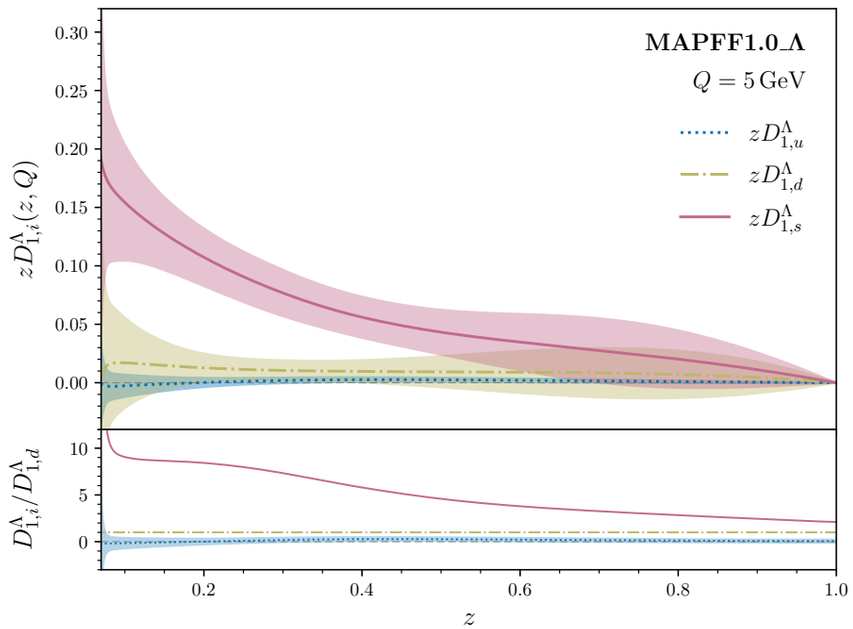

Summary

- Global analysis at next-to-next-to-leading order of perturbative accuracy of the **collinear unpolarised FFs for Λ hyperons**
- The fit is based on experimental data from SIA and both neutral-current and — for the first time — **charged-current SIDIS**.
- Statistical framework based on the Monte Carlo sampling method and FFs parameterisation in terms of a **neural network** that comprises a total of seven independent flavours.

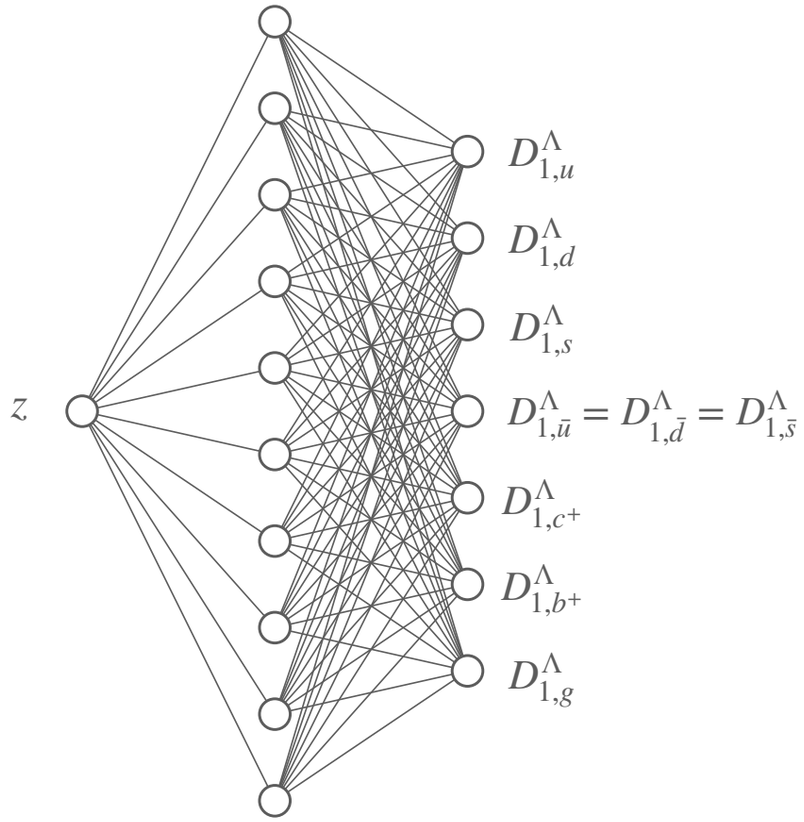

- First determination for the Λ and $\bar{\Lambda}$ **separately**, offering new insights into the hadronisation mechanism of strange baryons and establishing a baseline for future phenomenological investigations.

All results are obtained using the code available at
https://github.com/MapCollaboration/MontBlanc/tree/Lambda

The extracted FFs will be made available in the LHAPDF format as **MAPFF10NLOLambda** and **MAPFF10NNLOLambda**